

Chronostratigraphy of uplifted Quaternary hemipelagic deposits from the Dodecanese island of Rhodes (Greece)



Frédéric Quillévéré ^{a,*}, Jean-Jacques Cornée ^b, Pierre Moissette ^{a,c},
Gatsby Emperatriz López-Otalvaro ^{a,b}, Christiaan van Baak ^d, Philippe Münch ^b,
Mihaela Carmen Melinte-Dobrinescu ^e, Wout Krijgsman ^d

^a Univ Lyon, Université Lyon 1, ENS de Lyon, CNRS UMR 5276 LGL-TPE, F-69622 Villeurbanne, France

^b UMR5243 CNRS, Geosciences Montpellier, Université Montpellier 2, 34095 Montpellier Cedex 05, France

^c Department of Historical Geology-Paleontology, University of Athens, Panepistimiopolis, 15784 Athens, Greece

^d Paleomagnetic Laboratory "Fort Hoofddijk", Utrecht University, Budapestlaan 17, 3584 CD, Utrecht, The Netherlands

^e National Institut of Marine Geology and Geoeontology, 23-25 Dimitrie Onciu Street, PO Box 34-51, 70318 Bucharest, Romania

ARTICLE INFO

Article history:

Received 14 January 2016

Keywords:

Nannofossils

Foraminifera

Biostratigraphy

Magnetostratigraphy

⁴⁰Ar/³⁹Ar dating

Quaternary

Rhodes

Eastern Mediterranean

ABSTRACT

An integrated magneto-biostratigraphic study, based on calcareous nannofossils and foraminifers, together with the radiometric dating of a volcaniclastic layer found in several outcrops, was carried out on the hemipelagic deposits of the *Lindos Bay Formation* (LBF) at six localities on the island of Rhodes (Greece). Our highly refined chronostratigraphic framework indicates that the lower and upper lithostratigraphic boundaries of the LBF are diachronous. Associated with the ⁴⁰Ar/³⁹Ar age determination of 1.85 ± 0.08 Ma for the volcaniclastic layer, our data show that among the investigated outcrops, the Lindos Bay type locality section provides the longest record (1.1 Ma) of the LBF. Hemipelagic deposition occurred continuously from the late Gelasian (~1.9 Ma) to the late Calabrian (~0.8 Ma), i.e., from Chrons C2n (Olduvai) to C1r.1r (Matuyama) and from nannofossil Zones CNPL7 to CNPL10. This long record, together with the hemipelagic nature of the deposits, make the Lindos Bay type locality section a unique element in the eastern Mediterranean region, allowing future comparisons with other early Quaternary deep-sea sections available in the central and western Mediterranean regions.

© 2016 University of Washington. Published by Elsevier Inc. All rights reserved.

Introduction

In the central Mediterranean, the subduction of the Ionian crust beneath Eurasia has contributed to the uplift of Quaternary hemipelagic sedimentary sequences now exposed onshore along the Calabrian and Hellenic fore-arcs (e.g., Lourens et al., 1996; Papanikolaou et al., 2011). Located at coastlines and on islands of the Ionian Sea, these sequences have been of immense assistance for our understanding of the tectonic and climatic evolution of the Mediterranean (e.g., Massari et al., 2002). Some of them, in particular in Calabria and Sicily, now formally serve as global stratotype sections and points (GSSPs) for the Quaternary system (e.g., Gibbard et al., 2010; Cita et al., 2012). In the Aegean Sea, some uplifted Quaternary marine sedimentary successions occur in Crete

(Tortorici et al., 2010), Karpathos (Barrier et al., 1979) and Kos (Drinia et al., 2010) but none of these exhibit hemipelagic facies comparable to those available from the Ionian Sea. On the Dodecanese island of Rhodes (Greece) in the easternmost part of the Hellenic fore-arc, however, such deep-water deposits outcrop onshore. Although their chronostratigraphy is still a matter of debate (Titschack et al., 2013; see below), these deposits are well exposed, easily accessible, very fossiliferous and have the potential to be amenable for future comparisons with sequences available in the central and western Mediterranean regions.

The tectonic and sedimentary evolution of Rhodes has been investigated for several decades because of its significance for reconstructing the geodynamic history of the Hellenic sedimentary fore-arc (Meulenkamp et al., 1972; Pirazzoli et al., 1989; Duermeijer et al., 2000; Ten Veen and Kleinspehn, 2002). Since the Pleistocene, Rhodes was affected by tectonics controlled by major N 70° trending sinistral strike-slip faults, anticlockwise rotation and important vertical motions (e.g., Benda et al., 1977; Flemming and Woodworth, 1988; Hanken et al., 1996; Cornée et al., 2006a; van

* Corresponding author. Laboratoire de Géologie de Lyon, Université Lyon 1, 69622 Villeurbanne, France.

E-mail address: federic.quillevere@univ-lyon1.fr (F. Quillévéré).

Hinsbergen et al., 2007; Ten Veen et al., 2009). Such vertical motions have contributed to the uplift of Pleistocene deep-sea sedimentary sequences, now cropping out on the eastern coast of the island (Fig. 1). These deposits rest upon a deformed and deeply eroded, mainly calcareous Mesozoic basement (Mutti et al., 1970; Lekkas et al., 2001). The multiple faulting of this basement has generated a series of steep horsts and grabens that later conditioned the nature and distribution of the Pleistocene deposits (Hanken et al., 1996). Within the separate grabens, sedimentary facies changes are common. Despite recent advances relying on a range of approaches including bio-, magneto-stratigraphy and/or radioisotope dating (Thomsen et al., 2001; Cornée et al., 2006a, 2006b; Titschack et al., 2013), correlations between separated infillings are difficult to establish and the chronostratigraphy of these marine deposits is consequently still poorly understood.

The Pleistocene marine deposits of Rhodes have been shown to record a major, tectonically controlled transgressive-regressive cycle (Hanken et al., 1996; Kovacs and Spjeldnaes, 1999; Cornée et al., 2006a; Titschack et al., 2013), which reached bathyal depths during maximum transgression (Moissette and Spjeldnaes, 1995; Hanken et al., 1996). This promoted the deposition of the hemipelagic clays of the so-called *Lindos Bay Formation*, which crop out in numerous localities along the eastern coast of Rhodes. Because of their hemipelagic nature and the preservation, in particular, of calcareous nannofossils and planktonic foraminifera (Frydas, 1994; Beckman, 1995; Thomsen et al., 2001; Cornée et al.,

2006a, 2006b), these uplifted deposits constitute a key target for identifying bio-events that can be used to correlate between sections of the island and estimate their age and timing of deposition.

The present study aims to resolve the chronostratigraphy of these deposits. On the basis of biostratigraphic analyses (calcareous nannofossils and foraminifers) combined with magnetostratigraphy and $^{40}\text{Ar}/^{39}\text{Ar}$ dating of a volcaniclastic tuff, we generate firm chronological constraints for the *Lindos Bay Formation* type locality section. Comparisons with new and previously published stratigraphic data from other isolated sections distributed along the eastern coast of Rhodes (e.g., Thomsen et al., 2001; Cornée et al., 2006a, 2006b; Titschack et al., 2013) allow us to better document the sedimentary evolution of Rhodes. Such a previously poorly known hemipelagic succession exposed on land is finally elevated to a level where it can serve as a useful archive for reconstructing the tectonic, environmental and climatic changes that occurred in the Mediterranean region during the Pleistocene.

Lithostratigraphic and chronostratigraphic background

Previous stratigraphic studies of the marine Pleistocene deposits of Rhodes have been conducted by Keraudren (1970), Mutti et al. (1970), Meulenkamp et al. (1972), Løvlie et al. (1989), Frydas (1994), Hanken et al. (1996), Nelson et al. (2001), Thomsen et al. (2001), Nielsen et al. (2006), Cornée et al. (2006a; 2006b) and Titschack et al. (2013). After Hanken et al. (1996), several lithostratigraphic schemes were proposed (Fig. 2) in which the marine deposits recording the major, tectonically-controlled Pleistocene transgressive-regressive cycle has been qualified as the *Rhodes Synthem* (Titschack et al., 2013). Below the *Rhodes Synthem*, the *Kritika Formation* (~180 m thickness) is composed of brackish to shallow marine siliciclastic deposits considered either as Piacenzian-Gelasian (Sissingh, 1972; Benda et al., 1977; Moissette et al., 2016) or Calabrian (Thomsen et al., 2001; Rasmussen et al., 2005). Within the *Rhodes Synthem*, the *Kolymbia Formation* (4–20 m thickness) is composed of lower offshore (~30–120 m paleo-water depth; Steinthorsdóttir et al., 2006) bioclastic limestones, which have been

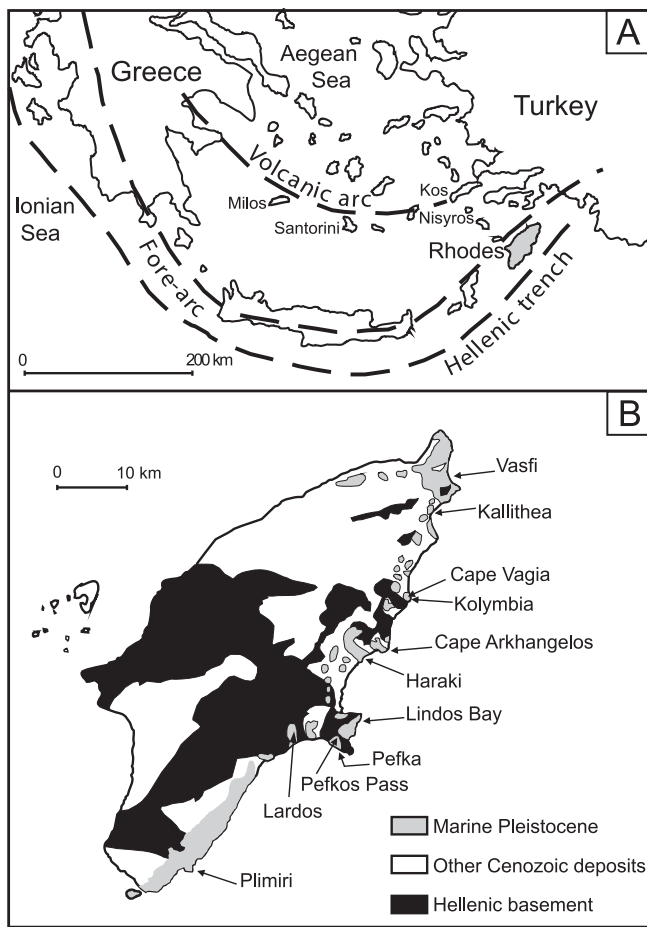


Figure 1. (A) Location map and geodynamic context of the island of Rhodes in the eastern Mediterranean (modified from Meulenkamp et al., 1972) and (B) simplified geological map of Rhodes (modified from Mutti et al., 1970), with location of the sections/outcrops of the *Lindos Bay Formation* studied or mentioned in this paper.

Eastern coast of Rhodes			
Hanken et al. (1996)	Cornée et al. (2006a)	Titschack et al. (2013)	Synthems
Kleopolu calcirudite GAB WBBB	Not studied	Plimiri Kleopolu Gialos WB	Lindos Acropolis
Cape Arkhangelos calcarenite SPBL clay ?	0.3 Ma Tsampika Ladiko 1.3 Ma Arkhangelos 1.4–1.3 Ma Ladiko sand Kolymbia HL	Tsampika Ladiko Cape Arkhangelos SPB Lindos Bay Kolymbia	< 0.35 Ma < 0.46 Ma
Kritika	Kolymbia 2 Ma	Kritika Damatria	Trianda
	Basement		

Figure 2. Comparison of lithostratigraphic schemes for the Pliocene and Pleistocene deposits of the eastern coast of Rhodes with associated published temporal landmarks. HL = Haraki Limestone, SPBL = Saint Paul's Bay Limestone, WBBB = Windmill Bay Boulder Bed, GAB = Gialos Algal Biolithite, SPB = Saint Paul's Bay, WB = Windmill Bay.

estimated as Piacenzian ([Løvlie et al., 1989](#)) or Gelasian ([Hanken et al., 1996; Cornée et al., 2006a](#)) or Gelasian to Calabrian ([Titschack et al., 2013](#)). The *Lindos Bay Formation* (LBF; 45 m maximum thickness; *Vasfi Formation* in [Meulenkamp et al., \(1972\)](#)), on which this study is focused, is composed of hemipelagic blue-grey calcareous to silty clays that record the most pronounced tectonic drowning of the eastern part of Rhodes, with a maximum paleo-water depth estimated at 300–600 m ([Moissette and Spjeldnaes, 1995](#)). Deposition of the LBF has been estimated to have occurred either from the Piacenzian to the Ionian ([Løvlie et al., 1989](#)), from the late Gelasian to the early Calabrian ([Cornée et al., 2006a, 2006b](#)), from the Calabrian to the early Ionian ([Titschack et al., 2013](#)) or during the late Calabrian ([Thomsen et al., 2001](#)). The *Saint Paul's Bay Formation* is a condensed lateral equivalent of the LBF that patchily outcrops south of the city of Lindos, in and near Saint Paul's Bay. It developed in contact with steep basement paleo-topography and contains abundant bathyal azooxanthellate corals, especially *Lophelia pertusa* ([Titschack and Freiwald, 2005](#)). The LBF is unconformably overlain by the pluri-facies *Cape Arkhangelos Formation* (up to 20–30 m thick), which indicates a major tectonic uplift of Rhodes and is estimated to have started eroding the LBF during the middle ([Hansen, 1999; Cornée et al., 2006a](#)) or late Calabrian to early Ionian ([Hanken et al., 1996; Titschack et al., 2013](#)). Finally, the overlying Pleistocene units are represented by the siliciclastic deposits of the *Ladiko-Tsampika Formation* and the limestone and sand facies of the *Lindos Acropolis Synthem* ([Cornée et al., 2006a; Titschack et al., 2008, 2013](#)).

Outcrops of the LBF have a patchy distribution along the eastern coast of Rhodes, from the locality of Vasfi in the north to that of Plimiri in the south ([Fig. 1](#)). Because they constitute erosional remnants, deposits exhibit extremely variable thicknesses. As pointed out by [Hanken et al. \(1996\)](#), many biostratigraphic markers that have been used, such as ostracods, sporomorphs, benthic foraminifers and bivalves ([Keraudren, 1970; Sissingh, 1972; Benda et al., 1977](#)), are strongly facies-controlled and may have influenced the interpretation of the analyzed isolated sections. Such discrepancies also originate from the steep and irregular paleo-topographies on which deposition occurred, resulting in markedly diachronous facies ([Hanken et al., 1996; Titschack et al., 2013](#)). A limited number of the studied sections exhibit an exposed lower boundary for the LBF (i.e., contact with the *Kolymbia Formation*). From north to south, such a contact outcrops at Cape Vagia, Cape Arkhangelos south, Lindos Bay, Pefka and Plimiri ([Fig. 1](#)). In all other sections with stratigraphic data, the contact is not exposed. This is for example the case at the 6.5 m

thick Haraki section ([Fig. 1](#)), where [Cornée et al. \(2006b\)](#) discovered an intercalated volcaniclastic layer. Based on the $^{40}\text{Ar}/^{39}\text{Ar}$ dating of this layer, together with magnetostratigraphic and planktonic foraminiferal data, these authors provided chronostratigraphic constraints demonstrating that part of the LBF was deposited during the Olduvai Subchron (1.945–1.778 Ma; [Hilgen et al., 2012](#)). Finally, because of the predominantly erosional top of the LBF, the age of its upper boundary varies considerably from section to section. As a consequence, the estimated duration of the interval during which the LBF was deposited (and then other lithostratigraphic units of the *Rhodes Synthem*) is extremely variable. At Lardos ([Fig. 1](#)), however, some muddy silts and sands have been attributed to the uppermost LBF. Here, $^{234}\text{U}/^{238}\text{U}$ radiogenic series measured on coral fragments of *L. pertusa* yielded an early Ionian age of ~756 ka and ~689 ka ([Titschack et al., 2013](#)).

Material and methods

Investigated sections and sampling

The present study describes for the first time a detailed chronostratigraphy of the *Lindos Bay Formation* type locality section ([Hanken et al., 1996](#)), located ~2 km north of the village of Lindos ([Fig. 1](#)). It also provides complementary information from other localities where the LBF is exposed in the areas of Cape Vagia, Cape Arkhangelos south, Pefka and Plimiri. Together with previously published data originating from the localities of Vasfi ([Orombelli and Montanari, 1967; Sissingh, 1972; Moissette and Spjeldnaes, 1995](#)), Kallithea ([Hansen, 1999; Thomsen et al., 2001; Cornée et al., 2006a; Lécuyer et al., 2012](#)), Haraki ([Cornée et al., 2006b](#)) and Lardos ([Titschack et al., 2013](#)), these sections allow us to compare records distributed along a NE–SW transect on the eastern coast of Rhodes ([Fig. 1](#)) and provide sufficient data to characterize the chronostratigraphy of the deposits.

The Lindos Bay type locality section ([Fig. 3](#); $36^{\circ}5'57''\text{N}$; $28^{\circ}5'12''\text{E}$) consists of ~5 m of *Kolymbia Formation* above present-day sea-level, and ~45 m of bluish-grey clays rich in pteropods, foraminifers, bivalves, scaphopods, brachiopods and bryozoans. Trace fossils (*Zoophycos*), corals (*Caryophyllia smithii*) and fish otoliths are common locally. The section provides the thickest LBF exposure on the island. The clays are generally massive, although they can be locally laminated and bioturbated. They exhibit a 14° NE dip (southern outcrop) that gently decreases northward



Figure 3. Field view and lithostratigraphy of the Lindos Bay type locality section, photographed from the southern side of the Lindos Bay.

(northern outcrop) and are capped by a ~8 m massive bryozoan-rich calcarenite with an erosive base characteristic of the *Cape Arkhangelos Formation*. Moissette and Spjeldnaes (1995) studied the bryozoan assemblages of the upper 28 m clays of the type locality section (northern outcrop; Fig. 3). They found that deposition occurred at depths of 300–500 m, with a shallowing to about 200–300 m in the top 4–5 m of the clays. Despite the remarkable thickness of the LBF in the Lindos Bay, and despite the section was erected as a type locality, no previous biostratigraphic and

magnetostratigraphic analyses were available there. For nannofossil and foraminiferal analyses, 26 samples (including 3 samples within the *Kolymbia Formation*) were collected with a sample spacing of ~1.7 m (Fig. 4). Within the same horizons, oriented hand samples were taken for magnetostratigraphy. During field investigation, an intercalated centimetre-thick volcaniclastic level (LIND-H) was discovered and sampled ~7 m above the top of the *Kolymbia Formation* (Fig. 3). This previously unrecognized layer corresponds to a crystal-tuff (*sensu* Cas and Wright, 1988) and exhibits the same

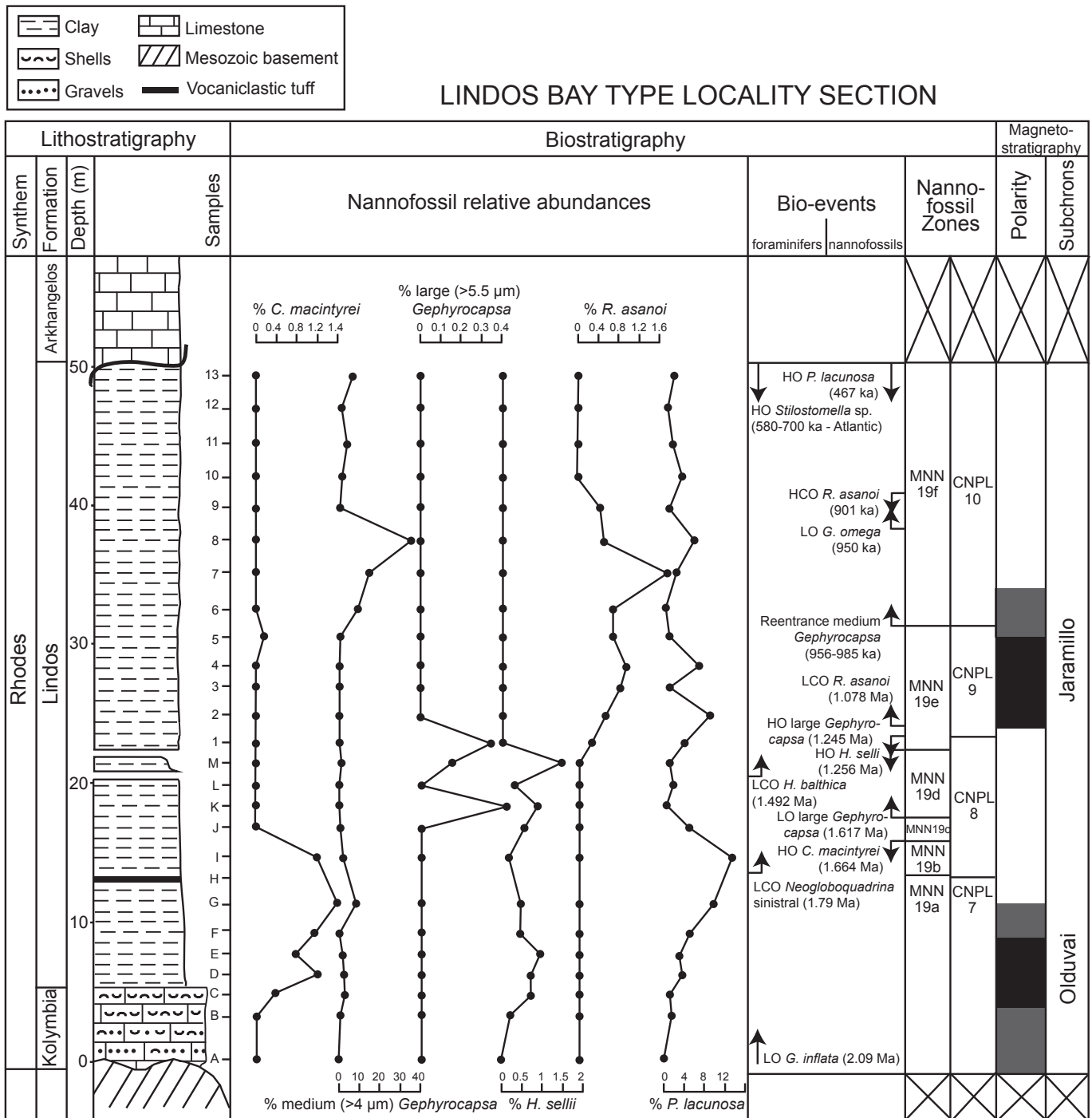


Figure 4. Lithostratigraphy, biostratigraphy and magnetostratigraphy of the deposits recovered from the Lindos Bay Clay type locality section. Tick marks show location of samples analyzed for biostratigraphy. The relative abundances of stratigraphically significant nannofossil taxa are shown throughout the section. Mediterranean foraminiferal and nannofossil bio-event calibrations follow [Lourens et al. \(2005\)](#) and [Raffi et al. \(2006\)](#), respectively. MNN and CNPL nannofossil zonal schemes are by [Rio et al. \(1990\)](#) and [Backman et al. \(2012\)](#), respectively.

mineralogy (amphibole, plagioclase and biotite) as the tuff present in the LBF of the Haraki section (Cornée et al., 2006b).

The contact between the *Kolymbia Formation* and the LBF is exposed in 4 other localities on the island, from north to south at Cape Vagia, Cap Arkhangelos south, Pefka and Plimiri (Fig. 1). The Cape Vagia section (Fig. 4; 36°14'98"N; 28°10'13"E) begins with ~6 m of *Kolymbia Formation* above present-day sea-level (Steinthorsdóttir et al., 2006). The LBF, which is unconformably capped by a strongly altered limestone (*Cape Arkhangelos Formation*), consists here of ~27 m of laminated to massive bluish-grey clays, rich in pteropods, bivalves, scaphopods, solitary corals, bryozoans, brachiopods, benthic and planktonic foraminifers and the trace fossil *Zoophycos* (Moissette and Spjeldnaes, 1995; Hanken et al., 1996; Bromley and Hanken, 2003). On the basis of bryozoan assemblages, a depth of 400 m–600 m was estimated for the deposition of the LBF, with a maximum depth recorded ~3 m above the *Kolymbia Formation* and a clear shallowing occurring near the top of the clays (Moissette and Spjeldnaes, 1995). We collected 26 samples (5 within the *Kolymbia Formation*) with an average sample spacing of ~1.3 m (Fig. 5) for biostratigraphic analyses, and used the magnetostratigraphy published by Cornée et al. (2006a). No volcanioclastic layer was found within the Cape Vagia section. Observations of thin sections within

the <5 mm reddish bed occurring ~1 m above the *Kolymbia Formation* (Fig. 5) and interpreted as an ash layer by Løvlie et al. (1989), showed that it is rather a ferruginous clayey deposit devoid of volcanic minerals (Cornée et al., 2006a). In the village of Kolymbia (Athens Street in front of the Atlantica Imperial Hotel; 36°15'11"N; 28°9'55"E, ~350 m W of the Cape Vagia Section, we found, however, a centimetre-thick volcanioclastic layer, intercalated within 2.5 m thick isolated LBF deposits where 4 additional samples were collected for biostratigraphy.

The Pefka section (Fig. 6) close to Plaka beach (36°3'49"N; 28°3'59"E) begins with ~9 m of *Kolymbia Formation* above present-day sea-level. The LBF consists of ~9 m of horizontal bluish-grey clay. The upper part of the section includes ~2 m of sand separated from the LBF by a firmground, and ~5 m of a shell-rich clayey limestone assigned to the *Cape Arkhangelos Formation*. For biostratigraphic analyses, 12 samples were collected (average sample spacing ~1.1 m within the LBF), including 3 samples in the *Kolymbia Formation* and 1 in the sand above the firmground (Fig. 6). We also found a centimetre-thick volcanioclastic layer in an isolated outcrop along the roadside of the Pefkos pass (36°4'38"N; 28°3'38"E), located at 80 m above sea level about 1.5 km NW of the Pefka section. This layer is intercalated within 3.5 m thick LBF

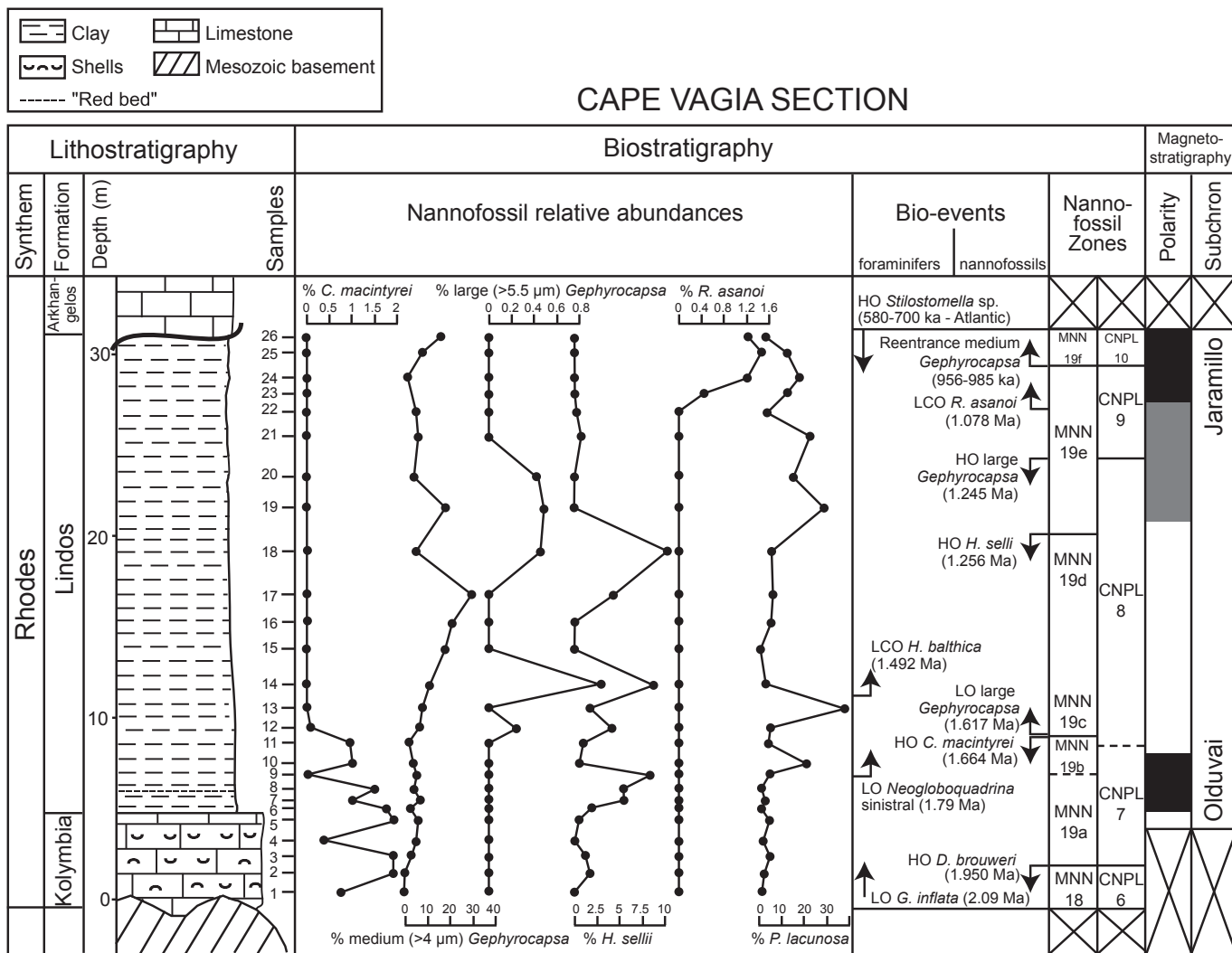
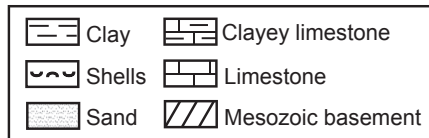


Figure 5. Lithostratigraphy, biostratigraphy and magnetostratigraphy (Cornée et al., 2006a) of the deposits recovered from the Cape Vagia section. Tick marks show location of samples analyzed for biostratigraphy. The relative abundances of stratigraphically significant nannofossil taxa are shown throughout the section. Mediterranean bio-event calibrations by Lourens et al. (2005) and Raffi et al. (2006). MNN and CNPL nannofossil zonal schemes by Rio et al. (1990) and Backman et al. (2012), respectively.



PEFKA SECTION

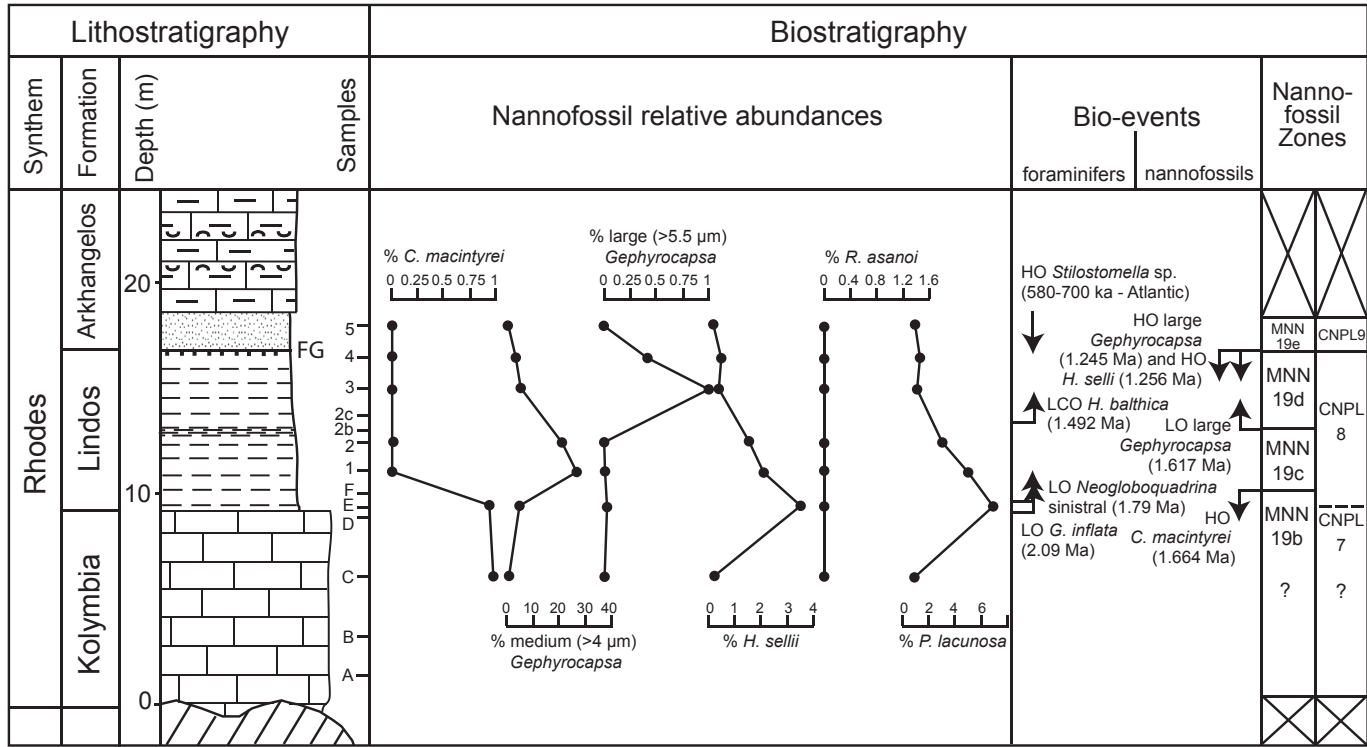


Figure 6. Lithostratigraphy and biostratigraphy of the deposits recovered from the Pefka section. Tick marks show location of samples analyzed for biostratigraphy. The relative abundances of stratigraphically significant nannofossil taxa are shown throughout the section. Mediterranean bio-event calibrations by Lourens et al. (2005) and Raffi et al. (2006). MNN and CNPL nannofossil zonal schemes by Rio et al. (1990) and Backman et al. (2012), respectively. FG = Firmground.

deposits where 5 additional samples were collected for biostratigraphy. Both volcaniclastic layers intercalated within the LBF in the isolated outcrops of Kolymbia and Pefkos also exhibit the hallmarks of the crystal tuff discovered at Haraki (Cornée et al., 2006b). However, it was not possible to determine their precise lithostratigraphic location within the LBF.

The Plimiri composite section (Fig. 7) consists of (1) ~4 m of LBF overlying ~2 m of sand and conglomerates probably belonging to the Kritika Formation and ~10 m of Kolymbia Formation for the southern outcrop ($35^{\circ}55'38''\text{N}$, $27^{\circ}51'44''\text{E}$) and (2) ~12 m of LBF for the northern outcrop ($35^{\circ}55'40''\text{N}$; $27^{\circ}51'46''\text{E}$). Both outcrops are unconformably capped by up to 10 m of limestone rich in red algae assigned to the Lindos Acropolis Synthem (Titschack et al., 2008, 2013). In the Plimiri composite section, 11 samples (including 4 within the Kolymbia Formation) were collected with an average spacing of 2.3 m (Fig. 7).

The Cape Arkhangelos south section ($36^{\circ}11'16''\text{N}$; $28^{\circ}7'25''\text{E}$) has not been sampled nor studied in this paper, but our field investigation revealed the occurrence of an intercalated volcaniclastic unit ~6 m above the top of the Kolymbia Formation, which also exhibits the same mineralogy as the crystal tuff discovered at Haraki (Cornée et al., 2006b).

Biostratigraphic analyses

For foraminiferal analyses, 84 samples were washed over a $65\ \mu\text{m}$ screen. The residue was dry-sieved and the size fractions coarser than

$125\ \mu\text{m}$ were used for foraminiferal analyses. Our biostratigraphic analysis is based on a complete inventory of planktonic foraminiferal species, following the taxonomic concepts and nomenclature of Kennett and Srinivasan (1983). Bio-event calibrations in the eastern Mediterranean are from Lourens et al. (2005). We also searched for the benthic foraminifers *Hyalinea balthica* and *Stilostomella* sp. These taxa are of stratigraphic significance, since *H. balthica* first commonly occurred in the Mediterranean after 1.492 Ma (Lourens et al., 1998) and *Stilostomella* sp. became extinct during the middle Pleistocene (Weinholz and Tutze, 1989; Kawagata et al., 2005), between 700 and 580 ka. Representatives of the most stratigraphically significant taxa were finally imaged with a SEM.

For calcareous nannofossil analyses, standard smear-slides were prepared. Depending upon preservation, a total of 300–500 coccoliths per sample were counted under an optical microscope (Zeiss Axioscop 40) at 1000x magnification. Pleistocene assemblages are dominated by gephyrocapsids and reticulofenestrids. Consequently, for taxonomic identification and owing to the taxonomic complexity of the genus *Gephyrocapsa* (Samtleben, 1980; Rio, 1982; Matsuoka and Okada, 1990; Bollmann, 1997), we adopted readily identifiable morphological features such as coccolith length, bridge angle and thickness, as described by Raffi et al. (1993) and Flores et al. (2000). To provide further information on the evolutionary range size variation of gephyrocapsids and reticulofenestrids, the length of the coccolith outlines was measured in both cross-polarized and bright fields. Coccolith images were finally captured using a CCD camera (Sony XC-77CE and MCCamera11

software). Measurements were performed with the Motic Images Plus 2.0 software. Lowest occurrences (LO), lowest common occurrences (LCO), highest occurrences (HO) and highest common occurrences (HCO) of stratigraphically significant taxa were extracted from the abundance patterns. The zonal subdivisions used by Rio et al. (1990) for the Plio-Pleistocene deposits of the western and central Mediterranean were followed. These subdivisions have proven applicable for the eastern Mediterranean, including Rhodes (Thomsen et al., 2001). The zonal scheme of Backman et al. (2012), applicable to the low and middle latitudes of the world oceans during the Pleistocene was also used. Calibration of nannofossil bio-event ages in the eastern Mediterranean is from Raffi et al. (2006).

Magnetostratigraphic analyses

Oriented hand samples from the Lindos Bay type locality section were collected at the levels sampled for biostratigraphy. These hand samples were drilled into standard-sized paleomagnetic specimens in the Paleomagnetic Laboratory "Fort Hoofddijk" of Utrecht University using compressed air. To

determine temperature steps for thermal demagnetization, thermomagnetic measurements were performed in air on a modified horizontal translation type Curie balance (noise level 5×10^{-9} Am²). After these analyses, samples were stepwise thermally demagnetized and magnetization was measured on a horizontal 2G Enterprises DC SQUID cryogenic magnetometer (noise level 3×10^{-12} Am²). Additional samples were demagnetized using alternating fields on a horizontal 2G Enterprises DC SQUID cryogenic magnetometer attached to an in-house built robotized sample handler controller.

⁴⁰Ar/³⁹Ar dating

Biotites and plagioclases were separated from the volcaniclastic layer sampled in the LBF of the Lindos Bay type locality section (sample LIND-H) in order to ensure the calibration of the paleomagnetic polarity scale. The sample was crushed and sieved. Grain size was in the order of 100–200 µm. Crystals were concentrated by using standard heavy liquid and/or a Frantz magnetic separator. The separated crystals were cleaned in 1 N nitric acid to dissolve possible carbonate impurities, then rinsed in successive ultrasonic

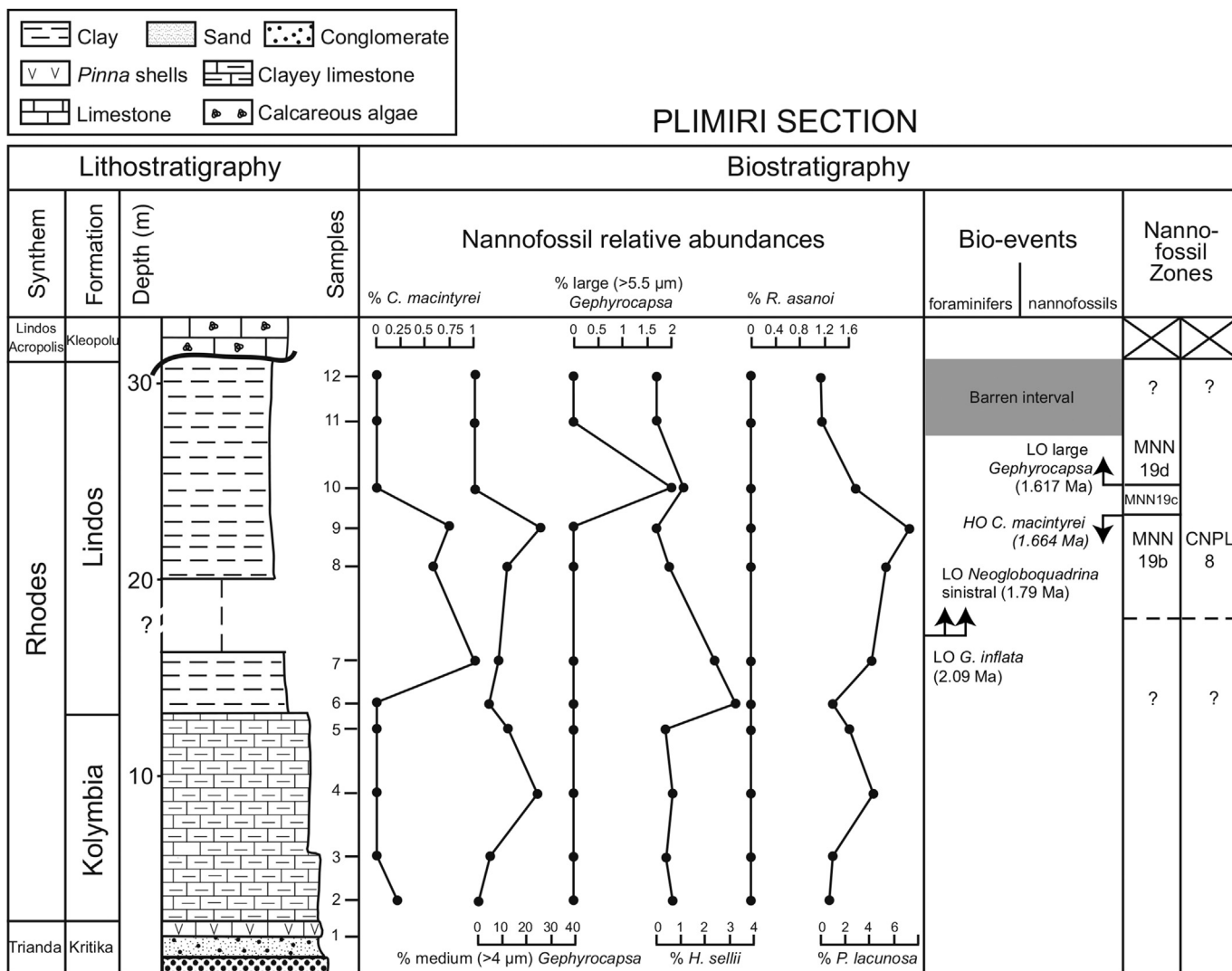


Figure 7. Lithostratigraphy and biostratigraphy of the deposits recovered from the Plimiri composite section. Tick marks show location of samples analyzed for biostratigraphy. The relative abundances of stratigraphically significant nannofossil taxa are shown throughout the section. Mediterranean bio-event calibrations by Lourens et al. (2005) and Raffi et al. (2006). MNN and CNPL nannofossil zonal schemes by Rio et al. (1990) and Backman et al. (2012), respectively.

baths of distilled water and pure alcohol. Finally, the grains were selected under a binocular microscope.

The sample was irradiated in the core of the Triga Mark II nuclear reactor at Pavia (Italy) with several aliquots of the Taylor Creek sanidine standard (28.34 ± 0.08 Ma; Renne et al., 1998) as a flux monitor. Argon isotopic interferences on K and Ca were determined by irradiation of KF and CaF_2 pure salts from which the following correction factors were obtained: $(^{40}\text{Ar}/^{39}\text{Ar})_{\text{K}} = 0.00969 \pm 0.00038$, $(^{38}\text{Ar}/^{39}\text{Ar})_{\text{K}} = 0.01297 \pm 0.00045$, $(^{39}\text{Ar}/^{37}\text{Ar})_{\text{Ca}} = 0.0007474 \pm 0.000021$ and $(^{36}\text{Ar}/^{37}\text{Ar})_{\text{Ca}} = 0.000288 \pm 0.000016$. Argon analyses were performed at Géosciences Montpellier (France) with an analytical device that consists of: (a) an IR-CO₂ laser of 100 kHz used at 3–15% power to heat samples during 60 s, (b) a lens system for beam focusing (a slightly defocused laser beam was used to yield a 0.4×0.4 mm beam of uniform intensity), (c) a steel chamber, maintained at $10^{-8} - 10^{-9}$ bar, with a copper holder in which 2 mm-diameter blind holes were milled, (d) an inlet line for purification of gases including two Zr-Al getters, and (e) a multi-collector mass spectrometer (Argus VI from Thermo-Fisher). Mass discrimination for the mass spectrometer was monitored by analyzing one air pipette volume and its measured values varied from 0.995588 ± 0.14 to 0.998418 ± 0.06 .

Aliquots of ten grains of biotite and of fifty grains of plagioclase were distributed one grain deep in one and two holes of the copper holder, respectively, and were step heated. Blank analysis were performed every three sample analyses. Raw data of each step and blank were processed and ages were calculated using the ArArCALC-software (Koppers, 2002). The criteria for defining plateau ages were: (1) plateau steps should contain at least 70% of released ^{39}Ar , (2) there should be at least three successive steps in the plateau and (3) the integrated age of the plateau should agree with each apparent age of the plateau within a 2σ confidence interval. All the subsequent quote

uncertainties are at the 2σ level including the error on the irradiation factor J.

Results

Biostratigraphy

In the Lindos Bay type locality section, planktonic foraminifers are abundant in all samples and their preservation ranges from moderate in the *Kolymbia Formation* to very good in the LBF (Fig. 8). A fauna of 22 taxa was documented, in which *Trilobatus sacculifer* (sensu André et al., 2013), *Globigerinoides ruber*, *Orbulina universa*, *Globigerina bulloides* and *Globigerinella siphonifera* constitute the most dominant taxa. As in many onland Quaternary successions from the Mediterranean, *Truncorotalia truncatulinoides* occurs very seldom (samples F and 9). *Globoconella inflata* (LO = 2.09 Ma) is continuously recorded within the *Kolymbia Formation* and LBF (Fig. 4). The LCO of *Neogloboquadrina sinistral* (1.79 Ma) correlates with the volcaniclastic layer. Finally, regarding benthic foraminifers (Fig. 8), the LCO of *Hyalinea balthica* (1.492 Ma) was identified while *Stilostomella* sp. occurs in most samples throughout the section.

Calcareous nannofossils are abundant and preservation is moderate to good (Fig. 9). Based on the occurrences and changes in relative abundances of biostratigraphically significant taxa (Fig. 4), from bottom to top of the section, we identified the HO of *Calcidiscus macintyreai* (1.664 Ma), the LO of large *Gephyrocapsa* ($>5.5 \mu\text{m}$; 1.617 Ma), the HO of *Helicosphaera sellii* (1.256 Ma), the LCO of *Reticulofenestra asanoi* (1.078 Ma), the reentrance datum of medium *Gephyrocapsa* ($\geq 4 \mu\text{m}$; 0.956–0.985 Ma) and the HCO of *R. asanoi* (0.901 Ma). Additional key information results from the LO of *Gephyrocapsa omega* (0.950 Ma; Cita et al., 2012) and the continuous occurrence of *Pseudoemiliana lacunosa* in all samples (Fig. 4). Altogether, these data show that the section spans the

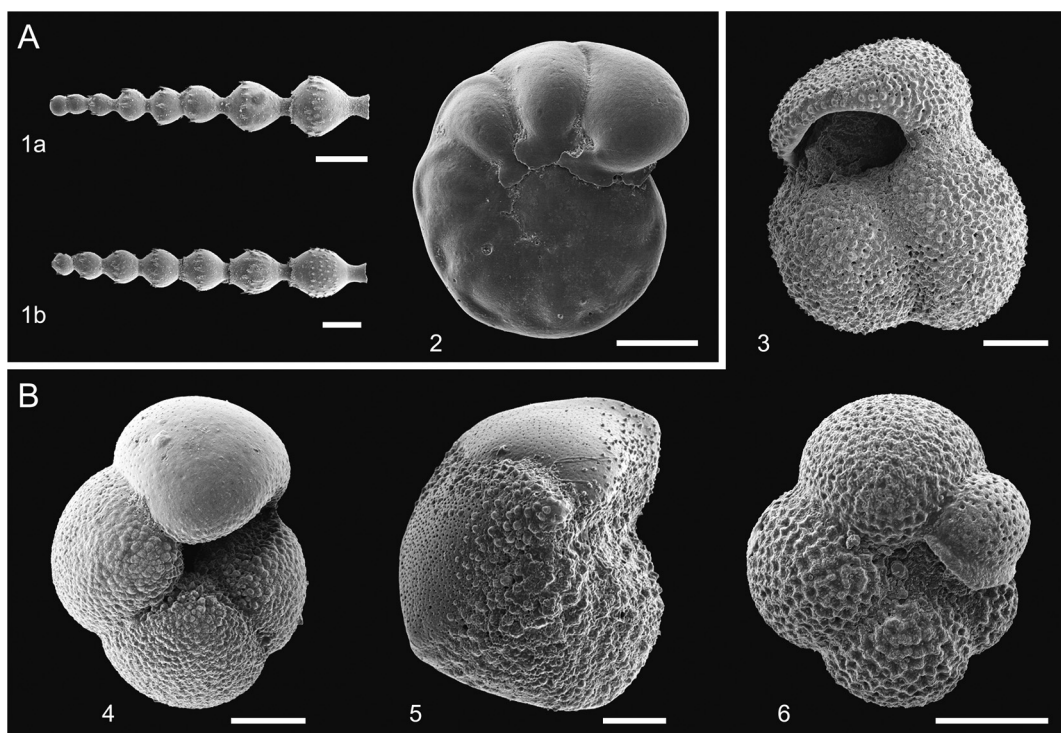


Figure 8. Scanning electron microphotographs of stratigraphically significant benthic (A) and planktonic (B) foraminifers from the *Lindos Bay Formation* in the Lindos Bay type locality section. 1: *Stilostomella* sp., samples M (a) and 4 (b). 2: *Hyalinea balthica* (Schröter), sample M. 3: *Globigerinoides extremus* Bolli and Bermudez, sample F. 4: *Globoconella inflata* D'Orbigny, sample 4. 5: *Truncorotalia truncatulinoides* (d'Orbigny), sample F. 6: *Neogloboquadrina sinistral*, sample I. Scale bar = $100 \mu\text{m}$.

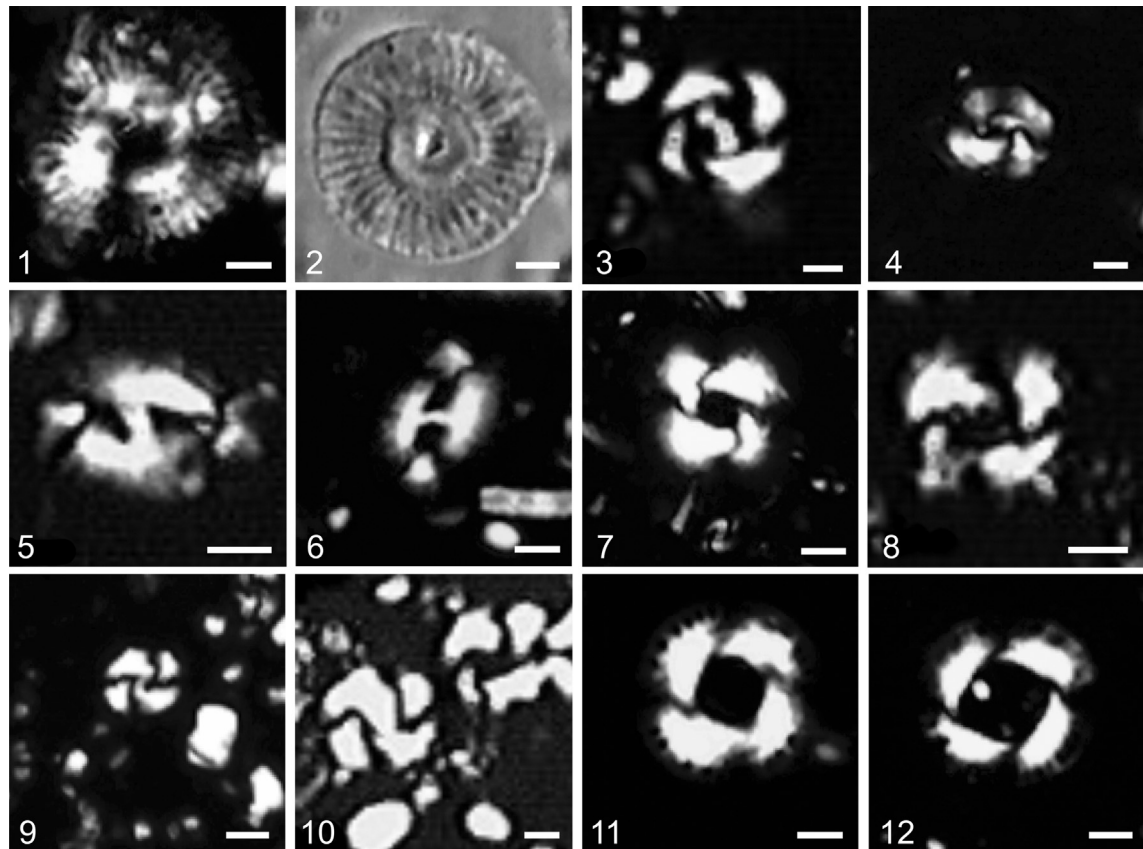


Figure 9. Microphotographs of stratigraphically significant calcareous nannofossil taxa from the *Lindos Bay Formation*. Scale bar = 2 μ m. All microphotographs in N+ (crossed nicols), except 2 in parallel nicols. 1, 2: *Calcidiscus macintyreui* (Bukry and Bramlette) Loeblich and Tappan, samples D and 9 at Lindos Bay and Plimiri, respectively. 3, 4: Large *Gephyrocapsa* spp. from samples 14 and 20 at Cape Vagia, respectively. 5, 6: *Helicosphaera sellii* (Bukry and Bramlette) Jafar and Martini, samples 8 and 18 at Cape Vagia, respectively. 7, 8: *Reticulofenestra asanoi* Sato and Takayama, samples 6 and 23 at Lindos Bay and Cape Vagia, respectively. 9, 10: medium *Gephyrocapsa* spp., samples 12 and 26 at Lindos Bay and Cape Vagia, respectively. 11, 12: *Pseudoemiliana lacunosa* (Kamptner) Gartner, samples 2 and 10 at Lindos Bay, respectively.

Mediterranean Subzones MNN19a (the MNN19a/MNN19b zonal boundary being approximated based on the LCO of *Neogloboquadrina sinistral*) to MNN19f (Rio et al., 1990), which correlate with the low and middle latitudes Zones CNPL7 to CNPL10 of Backman et al. (2012).

Among the other sections sampled and analyzed for biostratigraphy, Cape Vagia yields the most complete zonal succession (Fig. 5). Planktonic foraminifers here are abundant, well preserved (except a barren sample 15) and assemblages are similar to those found at Lindos. *Globoconella inflata* and *Stilostomella* sp. are continuously recorded and the LO of *Neogloboquadrina sinistral* and the LCO of *H. balthica* were identified. Preservation of nannofossils ranges between poor to moderate in the entire section, except in samples 14 to 16 in which preservation is very poor due to dissolution. Foraminifer data, together with the HO of *Discoaster brouweri* (1.95 Ma), HO of *C. macintyreui*, LO of large *Gephyrocapsa* ($>5.5 \mu$ m), HO of *H. sellii*, HO of large *Gephyrocapsa* ($>5.5 \mu$ m), LCO of *R. asanoi* and reentrance of medium *Gephyrocapsa* ($\geq 4 \mu$ m), indicate that the Kolymbia-Lindos succession at Cape Vagia (Fig. 5) encompasses the Mediterranean Zones and Subzones MNN18 to MNN19f (Rio et al., 1990), which correlate with the low and middle latitudes Zones CNPL6 to CNPL10 of Backman et al. (2012).

At Kolymbia, ~350 m west of the Cape Vagia section, *G. inflata* and *C. macintyreui* co-occur in all samples below and above the volcanoclastic layer outcropping there, although preservation of nannofossils ranges between very poor to moderate.

At Pefka (Fig. 6), the lower part of the section lacks any biostratigraphic data, because preservation of planktonic foraminifers is poor in the *Kolymbia Formation*. It is however very good in LBF deposits. Here, *T. truncatulinoides* (LO = 2.00 Ma) occurs seldom in samples E, 4 and 5, *Stilostomella* sp. occurs throughout the section, and the LO of *Neogloboquadrina sinistral* and LCO of *H. balthica* were identified. Because of the poor preservation in the *Kolymbia Formation*, we note that *G. inflata* occurs within LBF only, but found this taxa in all samples collected at Pefkos pass, where a volcanoclastic ash layer was discovered. Nannofossils are well preserved in all samples, except again in those collected from the *Kolymbia Formation*, where preservation is moderate. The HO of *C. macintyreui* and the LO of large *Gephyrocapsa* ($>5.5 \mu$ m) are located between samples E and 1 and between samples 2 and 3 (Fig. 6), respectively. An unconformity is found to correlate with the firmground level, because of the juxtaposed HOs of large *Gephyrocapsa* ($>5.5 \mu$ m) and *H. sellii*. Although the biostratigraphy of the lower part of the section could not be established (Fig. 6), the Kolymbia-Lindos-Arkhangelos (sandy part) succession at Pefka discontinuously encompasses Subzones MNN19a to MNN19e (Rio et al., 1990), which correlate with Zones CNPL7 to CNPL9 (Backman et al., 2012).

Finally, at Plimiri (Fig. 7), the LBF of the composite section apparently covers Subzones MNN19b to MNN19d (Rio et al., 1990), which correlate with Zone CNPL8 (Backman et al., 2012), but biostratigraphic data are very scarce and ambiguous, and the lower part of the composite section (southern outcrop) lacks any biostratigraphic marker. In addition, there is a barren interval of

calcareous plankton occurring at the top of the northern section (samples 11 and 12; Fig. 7). *Globoconella inflata* and common *Neogloboquadrina sinistral* occur in the northern outcrop only. Nannofoams are well preserved in all samples that yielded calcareous plankton. *Discoaster triradiatus* (HO = 2.216 Ma) was found up to sample 8. On the other hand, the HO of *D. brouweri* and the HO of *C. macintyreai* co-occur in sample 9, suggesting that *Discoaster* species may be reworked, precluding any clear biostratigraphic interpretation of the southern outcrop (Kritika-Kolymbia-Lindos succession). Finally, specimens of large *Gephyrocapsa* (>5.5 µm) were found in sample 10 (Fig. 7).

Magnetostratigraphy

In the Lindos Bay type locality section, 24 samples were analyzed for magnetostratigraphy (Fig. 10). Upon heating, the thermomagnetic curves of most samples show a continuous decrease up to a maximum temperature of around 600 °C. Some curves show a significant increase in magnetization above 400 °C, indicating oxidation reactions forming magnetite (Fig. 10a, d). Stepwise demagnetization using alternating field and thermal methods results in half of the samples in consistent directions (Fig. 10b, c). Both normal and reverse polarities are determined. For part of the samples, especially where the thermal demagnetization shows reverse directions at temperatures above 200 °C, alternating field demagnetization results in intermediate directions (Fig. 10e, f). This is most likely the result of a partial overlap of two demagnetizing components. Therefore, in case of widely differing directions between thermal and alternating field demagnetized specimens from the same levels, the thermally demagnetized direction is preferred over the alternating field one.

Plotting all obtained thermal directions in a stereographic plot and separating the normal and reverse directions allow us to determine site mean directions (Fig. 10g). This is done by applying a maximum 45° cut-off angle. Both the mean normal and reverse directions show a ~20° counter-clockwise (ccw) vertical axis rotation compared to the expected geocentric axial dipole direction. This is in good agreement with the previously documented tectonic rotation of 17° ccw for Rhodes since 0.8 Ma (van Hinsbergen et al., 2007). A positive reversal test (McFadden and McElhinny, 1990) indicates that the two obtained means are statistically similar. We therefore have good confidence that the obtained paleomagnetic directions record the magnetization stored in the sediment at the time of deposition.

Although the total number of samples is relatively small ($n = 24$), four distinct polarity zones (two normal, two reverse) are present in the Lindos Bay type locality section (Fig. 10h). Using the biostratigraphic constraints, these zones can be correlated to the Global Polarity Timescale (Hilgen et al., 2012), with the two normal polarity zones correlating to Chrons C2n (Olduvai) and C1r.1n (Jaramillo).

$^{40}\text{Ar}/^{39}\text{Ar}$ geochronology

Results of $^{40}\text{Ar}/^{39}\text{Ar}$ analyses of biotite and plagioclase crystals collected from the volcaniclastic layer in the Lindos Bay type locality section (sample H in Fig. 4) are synthetized in Fig. 11.

The plagioclase bulk sample (#LindH_pl_23_t5) displays a plateau age of 1.80 ± 0.07 Ma corresponding to 97.88% of ^{39}Ar released. The inverse isochron ($^{36}\text{Ar}/^{40}\text{Ar}$ vs. $^{39}\text{ArK}/^{40}\text{Ar}$) for the plateau steps yields a concordant age of 1.83 ± 0.1 Ma (initial atmospheric $^{40}\text{Ar}/^{36}\text{Ar}$ ratio of 284 ± 31.9 , Mean Square Weighted Deviation [MSWD] = 0.51, Fig. 11). The initial $^{40}\text{Ar}/^{36}\text{Ar}$ ratio value is

indistinguishable from that of air (295.5) indicating that no extraneous argon is considered in the calculated age.

The small cluster of biotites (#LindH_Bi) displays a plateau age of 1.98 ± 0.04 Ma corresponding to 89.41% of ^{39}Ar released. The inverse isochron for the plateau steps yields a concordant age of 1.94 ± 0.06 Ma (initial atmospheric $^{40}\text{Ar}/^{36}\text{Ar}$ ratio of 356 ± 64.2 , MSWD = 0.45, Fig. 11). Thus the age obtained on the biotite cluster experiment is slightly older than the one obtained in the bulk plagioclase experiment and is not concordant with it. This might be related to the excess argon component of the biotite cluster experiment revealed by the high initial $^{40}\text{Ar}/^{36}\text{Ar}$ ratio value of the inverse isochron.

The plateau age of 1.80 ± 0.07 Ma is thus considered as the best estimate of the crystal tuff discovered in the Lindos Bay type locality section.

Discussion

Record of an explosive volcanic eruption during LBF deposition

The pyroclastic fallout initially documented by Cornée et al. (2006b) in hemipelagic deposits at Haraki can be documented elsewhere in the island. The age of the crystal tuff intercalated in the Lindos Bay type locality section (1.80 ± 0.07 Ma) is indeed fully concordant with the age of the tuff in the Haraki section (1.89 ± 0.09 Ma). This age is stratigraphically corroborated by the co-occurrence of *G. inflata* (LO = 2.09 Ma) and *C. macintyreai* (HO = 1.664 Ma) in sediments below and above the volcaniclastic tuff, very close to the LCO of *Neogloboquadrina sinistral* (1.79 Ma) and top of the Olduvai Subchron (1.778 Ma). This layer is associated with a reverse polarity in the Lindos Bay, just above samples attributed to the Olduvai Subchron, while the volcaniclastic layer at Haraki was recorded within the Olduvai Subchron. Because the age of these layers is identical, the reverse direction of samples G and H at Lindos Bay (Fig. 4) may have been acquired slightly later and after the reversal. This kind of delayed acquisition is relatively common in sedimentary rocks (e.g., van Hoof and Langereis, 1991; Vasiliev et al., 2008) and around reversals this may result in incorrect determination of the polarity. In addition, the top of the normal C2n (Olduvai) Chron shows multiple short-term directional changes and is therefore not the most accurate timeline (Hilgen, 1991). Moreover, the age of the volcaniclastic layers found in isolated outcrops of the LBF at Kolymbia near the Cape Vagia section and at Pefkos pass near the Pefka section can be constrained by using biostratigraphic data. In these two isolated outcrops, the crystal tuffs also fall in between the LO of *G. inflata* (2.09 Ma) and HO of *C. macintyreai* (1.664 Ma). Furthermore, the volcaniclastic layer at Cap Arkanghelos south was deposited ~6 m above the top of the *Kolymbia Formation*, similar to its position within the Lindos Bay type locality section. It is proposed that all these volcaniclastic layers correspond to a single volcanic event that can serve as a firm constraint for the chronostratigraphy of the lower part of the LBF. The weighted mean age of the concordant isochron ages in the Haraki and Lindos Bay type locality sections is 1.85 ± 0.08 Ma (2σ) and is retained as the best estimate of the age of the volcanic event responsible for pyroclastic minerals dispersion.

Because of its fore-arc location, it is thought that no volcanic activity has occurred on Rhodes since the Oligocene. The volcanic activity that occurred in the Aegean Sea since the Pliocene originates from the north of the Hellenic fore-arc only (Jolivet et al., 2013) and that occurring at Kos and Nisyros islands (about 100 km northwest of Rhodes; Fig. 1) during the early Pleistocene may explain the occurrence of the investigated volcaniclastic deposits within the LBF, as suggested by Cornée et al. (2006b). The crystal tuff deposited within the LBF may then be related to a huge

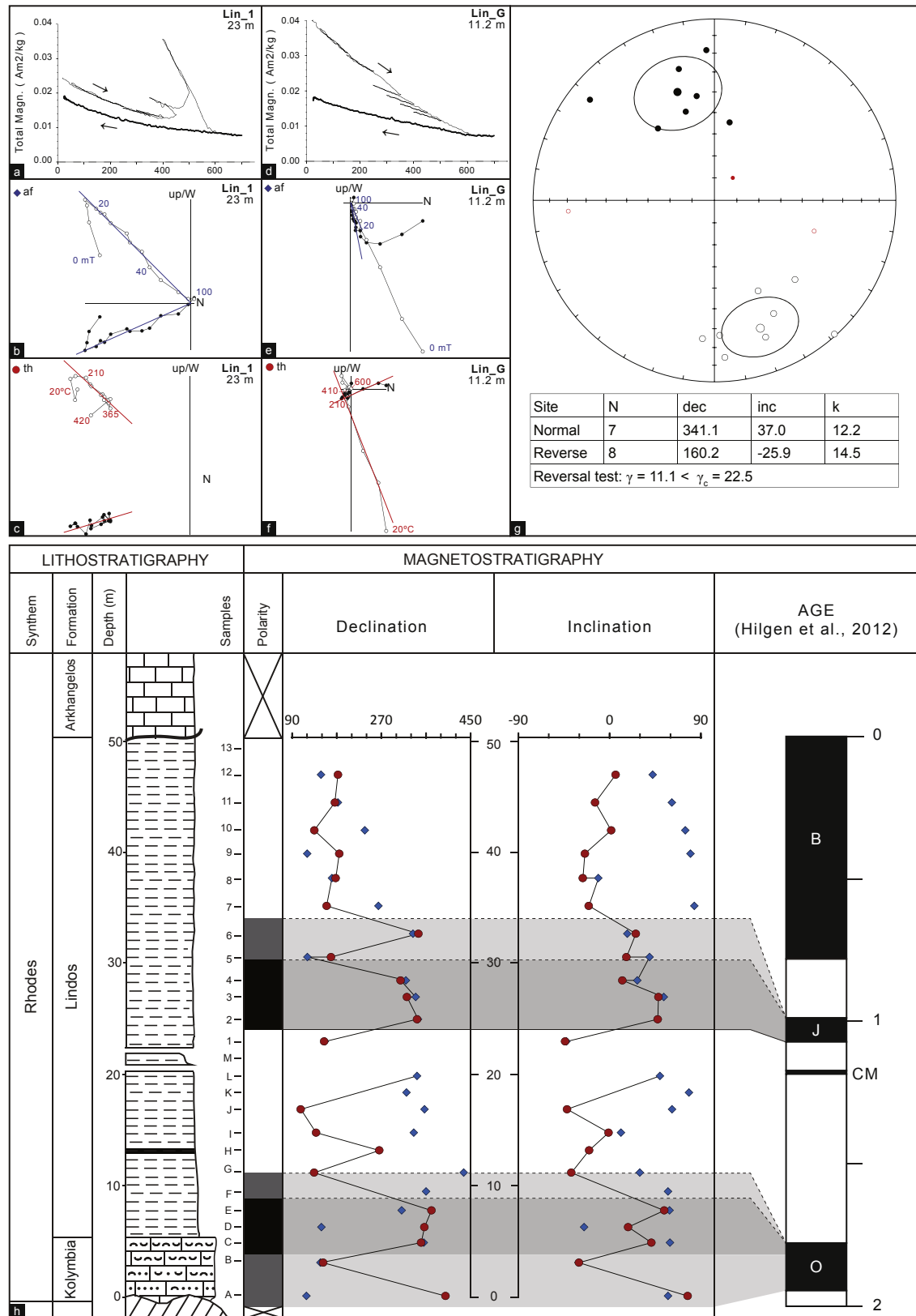


Figure 10. Magnetic parameters for samples 1 (a–c) and G (d–f) in the Lindos Bay type locality section. a,d) Thermomagnetic measurements; b,e) Orthogonal projections of stepwise alternating field (af) and c,f) thermal (th) demagnetization diagrams; g) equal area plot for thermal demagnetization data with N: number of samples, dec: mean declination, inc: mean inclination, k: precision parameter of Fisher (1953), γ and γ_c : the angle and critical angle determined by the statistics of the means; h) magnetostratigraphic results and correlation to the timescale, with red circles (blue diamonds) indicating the determined thermal (alternating field) directions. (For interpretation of the references to colour in this figure legend, the reader is referred to the web version of this article.)

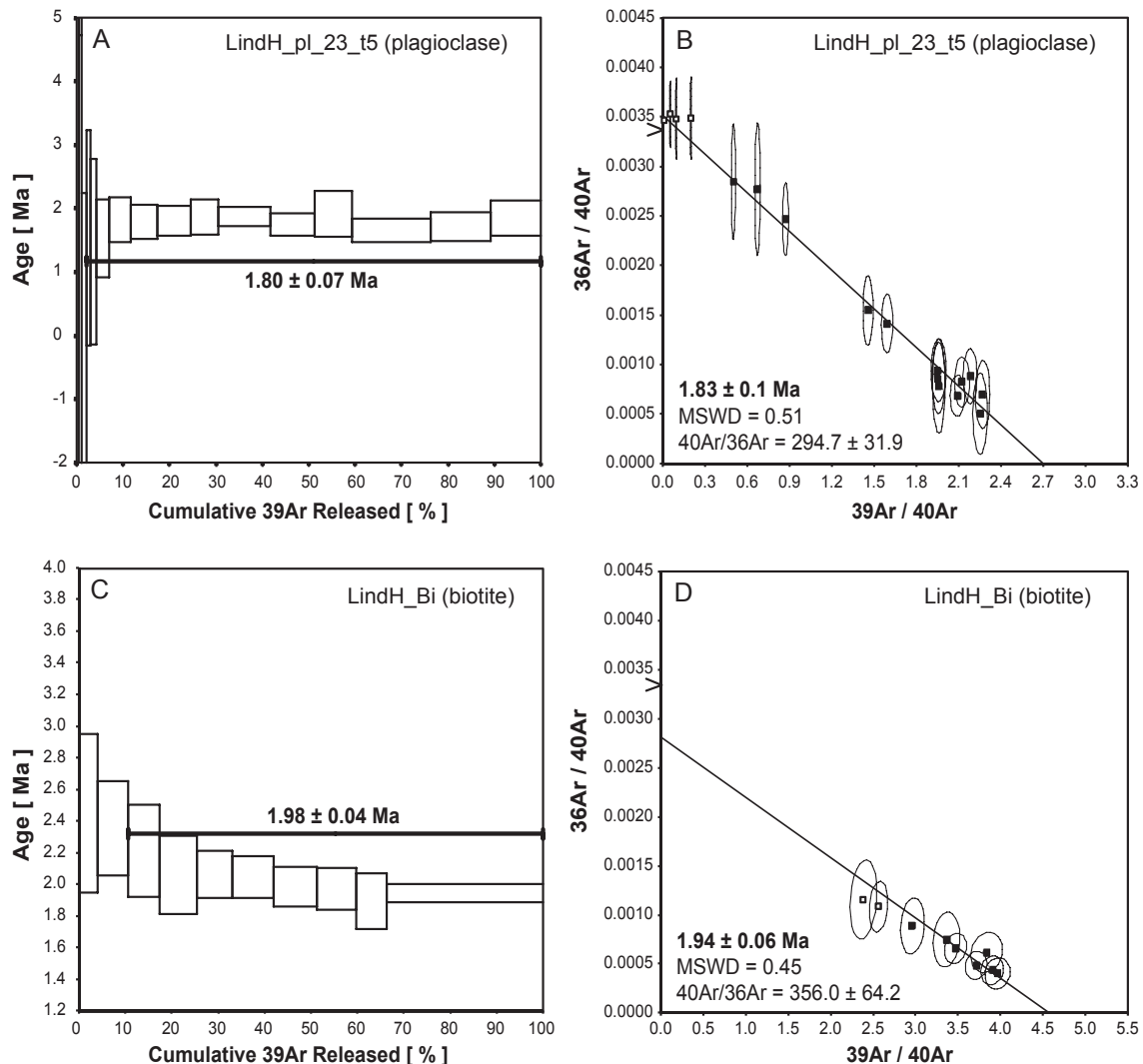


Figure 11. Sample #LindH degassing spectra for $^{40}\text{Ar}/^{39}\text{Ar}$ age analysis (A and C) and related inverse isochron diagrams (B and D, respectively). $^{40}\text{Ar}/^{36}\text{Ar}$ intercept values and MSWD are reported. Plain symbols correspond to steps used in plateau and inverse isochron calculations. Calculations are determined by using the ArArCALC-software of Koppers (2002).

explosive eruption at 1.85 Ma of the Nisyros–Yali–Kos volcanic system that was characterized by a dacite-andesite explosive volcanism in the early Pleistocene interval (DiPaola, 1974). Such a major eruption has also been proposed for the formation of a caldera between Kos and Nisyros in late Pleistocene times (Allen, 2001). However, a more distal origin, i.e., from the central part of the Aegean arc with Santorini and Milos Pliocene andesite-dacite volcanism (e.g., Bellon et al., 1979), cannot be completely ruled out as exemplified by the aerial distribution of Quaternary distal tephra in the eastern Mediterranean (Narcisi and Vezzoli, 1999).

Chronostratigraphy and diachronous nature of the Quaternary hemipelagic deposits of Rhodes

The chronostratigraphy of the studied uplifted Quaternary hemipelagic deposits of Rhodes is shown in Fig. 12. Because of the lack of biostratigraphic markers at Pefka and Plimiri in the south-eastern part of the island, information about the timing of deposition of the *Kolymbia Formation* is still limited. At Lindos Bay, the *Kolymbia Formation* was deposited after 2.09 Ma during the late Gelasian (LO of *G. inflata*), at a minimum during Subzone MNN19a and Zone CNPL7. At Cape Vagia, deposition of the *Kolymbia*

Formation started during Zones MNN18 and CNPL6 and continued during the early parts of Subzone MNN19a and Zone CNPL7. The onset of the deposition of the *Kolymbia Formation* therefore appears diachronous.

The lithostratigraphic boundary between the *Kolymbia Formation* and the LBF appears diachronous as well, from section to section along the eastern coast of Rhodes (Fig. 12). At oldest, deposition of the LBF occurred at Lindos Bay and Cape Vagia during the late Gelasian, within Subzone MNN19a and Zone CNPL7 close to the base of Chron C2n (Olduvai; 1.945 Ma). Southward, the age of the lower part of the LBF remains unknown at Plimiri, but it apparently occurs during the early Calabrian (~1.7 Ma) within Subzone MNN19b and close to the CNPL7/CNPL8 zonal boundary at Pefka. Finally, in the northernmost part of the island (Kallithea section), nannofossil analyses by Thomsen et al. (2001) revealed that the early Calabrian (Subzones MNN19a to MNN19e) is represented by clayey to conglomeratic littoral facies. There, the classical hemipelagic clayey facies of the LBF was deposited later during the late Calabrian, within Zone MNN19e (~1.1 Ma), a configuration that resembles that of Vasfi in the northernmost part of Rhodes (Orombelli and Montanari, 1967). Such a diachronous nature of the *Kolymbia Formation* and lower

part of the LBF corroborates previous results by Hanken et al. (1996) and Titschack et al. (2013), who highlighted the very high degree of diachroneity of the Quaternary lithostratigraphic units of Rhodes (Fig. 2), caused by their preservation in small independent canyon systems in which variable altitudes along proximal to distal transects conditioned the diachronous deposition of similar sedimentary facies.

Furthermore, it appears that among the investigated sections, the Lindos Bay type locality section exhibits the youngest deposits of the LBF (Fig. 12). Hemipelagic sediments available there deposited up to the late Calabrian within Subzone MNN19f and Zone CNPL10 and within Chron C1r.1r (Mutuyama), after the HCO of *R. asanoi* (901 ka) and before the base of Chron C1n (Brunhes, 781 ka; Hilgen et al., 2012). Because of the erosional nature of the contact

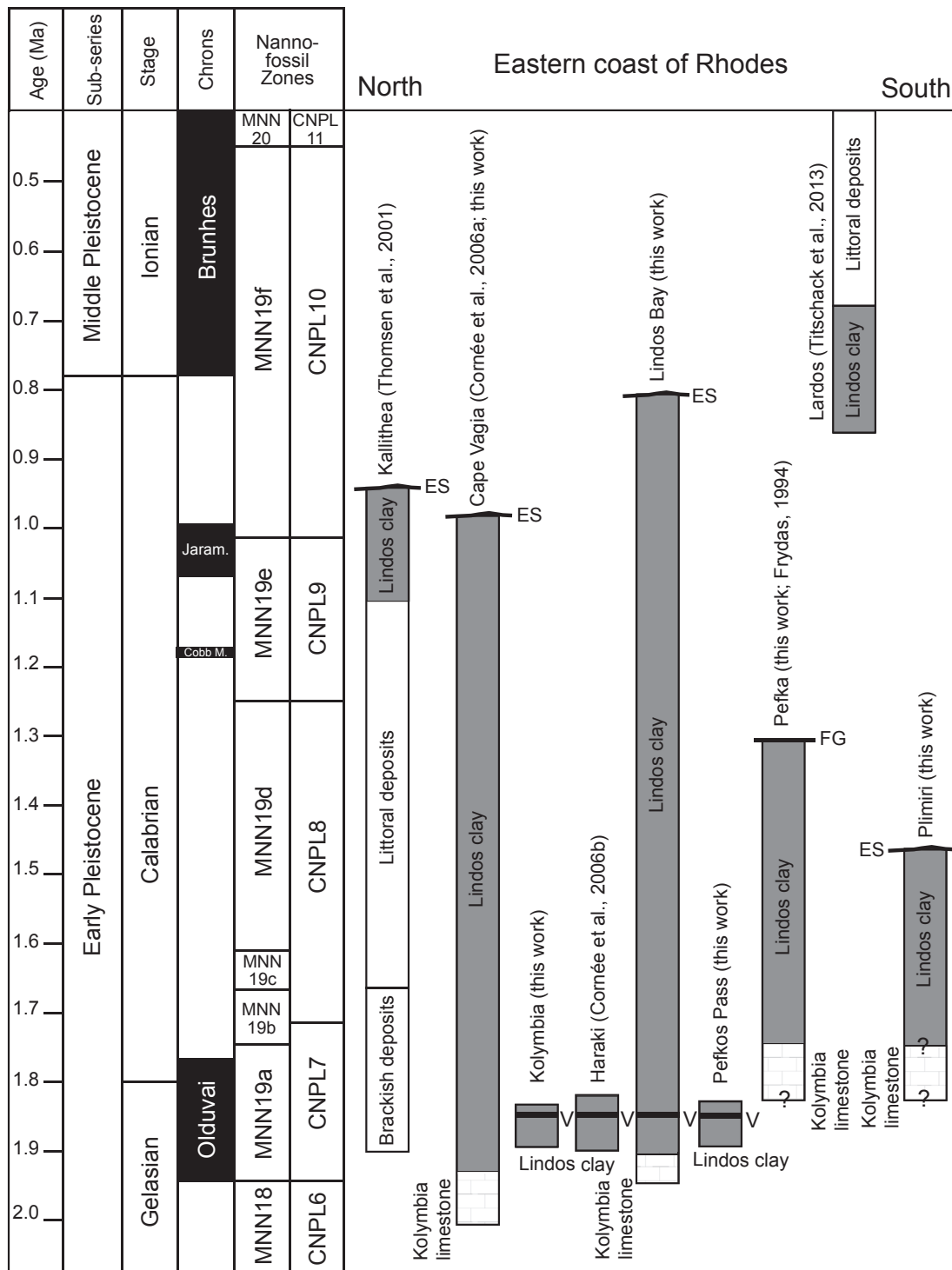


Figure 12. Compilation of chronostratigraphic data available from sections where the LBF outcrops in the eastern coast of Rhodes. Time scale from [Hilgen et al. \(2012\)](#) and calcareous nannofossil zonal schemes by [Rio et al. \(1990\)](#) and [Backman et al. \(2012\)](#) for the Mediterranean region and the low to middle latitudes of the world oceans, respectively. ES = Erosional surface, FG = Firmground, V = Volcaniclastic layer.

with overlying deposits (*Cape Arkhangelos Formation* at Cape Vagia and Pefka, *Kleopulu Formation* at Plimiri; Fig. 12), the top of the LBF outcropping in the other studied sections is clearly incomplete, diachronous and older. Northward at Cape Vagia, it correlates with Chron C1n.1r (Jaramillo) in the early part of Subzone MNNF19f and Zone CNPL10, similarly to the Kallithea section (Thomsen et al., 2001). Southward at Pefka and Plimiri, it correlates with Subzone MNN19d and Zone CNPL8 (early Calabrian). These data indicate that none of the investigated sections exhibit LBF deposits as young as those available from the lower part of the ~9 m thick Lardos section (Fig. 12). There, the upper part of the section is composed of silty and sandy sediments, much enriched in littoral fossils (e.g., *Glycymeris*, *Ditrupa*, rhodoliths; personal observation), which were deposited at shallower depths than the LBF. The muddier lower part of the section, however, yielded coral fragments of *Lophelia pertusa* dated up to ~689 ka (Titschack et al., 2013). This suggests that hemipelagic conditions still prevailed in several canyon systems of the eastern coast of Rhodes during the early Ionian at least in the early Chron C1n (Brunhes), and that the upper part of the Lindos Bay type locality section has been eroded prior to the deposition of the *Cape Arkhangelos Formation*.

Despite apparent erosion of its younger hemipelagic deposits, the Lindos Bay type locality section (and to a lesser degree the Cape Vagia section) exhibits a remarkably long temporal record of uplifted Quaternary hemipelagic sediments, from the late Gelasian (~1.9 Ma) to the late Calabrian (~0.8 Ma). It continuously records ~1.1 Ma of the Quaternary, from Chrons C2n (Olduvai) to Chron C1r.1r (Matuyama) and from calcareous nannofossil Zones CNPL7 to CNPL10. This result has significant implications for the ages of the overlying lithostratigraphic units, for which chronostratigraphic data are especially rare because of their shallow-water nature. Cornée et al. (2006a) proposed an age between 1.4 Ma and 1.3 Ma for the *Cape Arkhangelos Formation* and a time span between 1.3 Ma and 300 ka for the deposition of the *Tsampika-Ladiko Formation* (Fig. 2). Since these formations unconformably cover the LBF, such proposed ages appear incompatible with the results obtained here from the LBF and those obtained by Titschack et al. (2013) at Lardos (Fig. 2), and indicate that further geomorphologic, sedimentary and chronostratigraphic analyses will be needed to build a final depositional interpretation of the late Quaternary shallow-water deposits of Rhodes.

Conclusions

In the eastern part of the Mediterranean, a series of Quaternary marine deposits occurs onshore in the islands of Kephalonia (Keraudren, 1970), Zakynthos (Papanikolaou et al., 2011), Crete (Tortorici et al., 2010), Kos (Drinia et al., 2010) and Karpathos (Barrier et al., 1979). None of these deposits, however, have recorded deep-sea environments such as those uplifted along the eastern coast of the Dodecanese island of Rhodes. Our detailed, integrated calcareous nannofossil, foraminiferal and magneto-biostratigraphic analyses of these deposits, together with the $^{40}\text{Ar}/^{39}\text{Ar}$ age determination of 1.85 ± 0.08 Ma for a volcanoclastic layer found in five sections on the island, allows the chronostratigraphic calibration of the major, tectonically controlled transgressive-regressive cycle (*Kolymbia-Lindos-Arkhangelos Formations* succession) that led to the deposition of these hemipelagic deposits during the interval of maximal transgression (*Lindos Bay Formation*). Although the modalities of the deepening of the eastern part of Rhodes within the context of the Hellenic subduction remain to be estimated, we confirm that these hemipelagic deposits are highly diachronous from section to section, as a result of deposition in independent steep and irregular canyons, which developed at different altitudes along the eastern coast of Rhodes (Titschack

et al., 2013). Among the investigated outcrops, the Lindos Bay type locality section, for which no previous magneto-biostratigraphic data were available, exhibits the thickest (~45 m) and longest (1.1 Ma) onshore record of the *Lindos Bay Formation*, likely continuously from the late Gelasian (~1.9 Ma) to the late Calabrian (~0.8 Ma). This makes the Lindos Bay type locality section a unique element in the eastern Mediterranean region, allowing to compare its hemipelagic deposits with other Calabrian deep-sea sections available in western and central Mediterranean (e.g., Calabria, Sicily), and be amenable, in particular, for future high-resolution paleoenvironmental and paleoclimatic research.

Acknowledgments

We are thankful to Efterpi Koskeridou and Konstantina Agiadi who participated in the fieldwork, Sébastien Joannin and José-Abel Flores for helpful discussions. We also thank two anonymous reviewers and the Senior Editor Nicholas Lancaster who provided constructive comments that helped us to improve the present manuscript. This work was partly supported by a grant from the INSU SYSTER program (JJC).

References

- Allen, S.R., 2001. Reconstruction of a major caldera-forming eruption from pyroclastic deposit characteristics: Kos Plateau Tuff, eastern Aegean Sea. *Journal of Volcanology and Geothermal Research* 105, 141–162.
- André, A., Weiner, A., Quillévéré, F., Aurahs, R., Morard, R., Douady, C.J., de Garidel-Thoron, T., Escarguel, G., de Vargas, C., Kucera, M., 2013. The cryptic and the apparent reversed: lack of genetic differentiation within the morphologically diverse plexus of the planktonic foraminifer *Globigerinoides sacculifer*. *Paleobiology* 39 (1), 21–39.
- Barrier, E., Müller, C., Angelier, J., 1979. Sur l'importance du Quaternaire ancien marin dans l'île de Karpathos (arc hellénique, Grèce) et ses implications tectoniques. *Comptes-rendus de la Société Géologique de France* 4, 198–201.
- Backman, J., Raffi, I., Rio, D., Fornaciari, E., Pälike, H., 2012. Biozonation and biochronology of Miocene through Pleistocene calcareous nannofossils from low and middle latitudes. *Newsletters on Stratigraphy* 45, 221–224.
- Beckman, L.J., 1995. Stratigraphical and Sedimentological Investigations of Pliocene/Pleistocene Deposits at Lindos Bay, Rhodes. Unpublished Ph. D. thesis. University of Tromsø.
- Bellon, H., Jarrige, J.J., Sorel, D., 1979. Les activités magmatiques égées à l'Oligocène à nos jours et leurs caractères géodynamiques. Données nouvelles. *Revue de Géographie Physique et de Géologie Dynamique* 21, 41–55.
- Benda, L., Meulenkamp, J.E., van de Weerd, A., 1977. Biostratigraphic correlations in the eastern Mediterranean Neogene: 3. Correlation between mammal, sporomorph and marine microfossil assemblages from the Upper Cenozoic of Rhodes, Greece. *Newsletters on Stratigraphy* 6, 117–130.
- Bollmann, J., 1997. Morphology and biogeography of *Gephyrocapsa cocciliths* in Holocene sediments. *Marine Micropaleontology* 29, 319–350.
- Bromley, R.G., Hanken, N.-M., 2003. Structure and function of large, lobed *Zoothycos*: Pliocene of Rhodes, Greece. *Palaeogeography, Palaeoclimatology, Palaeoecology* 192, 79–100.
- Cas, R.A.F., Wright, J.V., 1988. *Volcanic Successions, Modern and Ancient*. Unwin Hyman Ltd, p. 487.
- Cita, M.B., Gibbard, P.L., Head, M.J., The ICS Subcommission on Quaternary Stratigraphy, 2012. Formal ratification of the GSSP for the base of the calabrian stage (second stage of the Pleistocene series, Quaternary system). *Episodes* 35 (3), 388–397.
- Cornée, J.-J., Moissette, P., Joannin, S., Suc, J.-P., Quillévéré, F., Krijgsman, W., Hilgen, F., Koskeridou, E., Münch, P., Lécuyer, C., Desvignes, P., 2006a. Tectonic and climatic controls on coastal sedimentation: the Late Pliocene-Middle Pleistocene of northeastern Rhodes, Greece. *Sedimentary Geology* 187, 159–181.
- Cornée, J.-J., Münch, P., Quillévéré, F., Moissette, P., Vasiliev, I., Krijgsman, W., Verati, C., Lécuyer, C., 2006b. Timing of Late Pliocene to Middle Pleistocene tectonic events in Rhodes (Greece) inferred from magneto-biostratigraphy and $^{40}\text{Ar}/^{39}\text{Ar}$ dating of a volcanoclastic layer. *Earth and Planetary Science Letters* 250, 281–291.
- DiPaola, G.M., 1974. Volcanology and petrology of Nisyros Island Dodecanese, Greece. *Bulletin of Volcanology* 38, 944–987.
- Drinia, H., Koskeridou, E., Antonarakou, A., Tzortzaki, E., 2010. Benthic foraminifera associated with the zooxanthellate coral *Cladocora* in the Pleistocene of the Kos island (Aegean Sea, Greece): sea level changes and palaeoenvironmental conditions. *Bulletin of the Geological Society of Greece* 43 (2), 613–619.
- Duermeijer, C.E., Nyst, M., Meijer, P.T., Langereis, C.G., Spakman, W., 2000. Neogene evolution of the Aegean Arc; paleomagnetic and geodetic evidence

- for a rapid and young rotation phase. *Earth and Planetary Science Letters* 176, 509–525.
- Fisher, R.A., 1953. Dispersion on a sphere. In: *Proceedings of the Royal Society of London, Series A*, 217, pp. 295–305.
- Flemming, N.C., Woodworth, P.L., 1988. Monthly mean sea levels in Greece during 1969–1983 compared to relative vertical movements measured over different timescales. *Tectonophysics* 148, 59–72.
- Flores, J.-A., Gersonde, R., Sierra, F.J., Niebler, H.-S., 2000. Southern ocean Pleistocene calcareous nannofossil events: calibration with the isotope and geomagnetic stratigraphies. *Marine Micropaleontology* 40 (4), 377–402.
- Frydas, D., 1994. Die Pliozän/Pleistozän-Grenze auf der Insel Rhodos (Griechland). *Müntersche Forschungen zur Geologie und Paläontologie* 76, 331–344.
- Gibbard, P.L., Head, M.J., Walker, M.J.C., Subcommission on Quaternary Stratigraphy, 2010. Formal ratification of the Quaternary system/epoch and redefinition of the Pleistocene series/epoch with a base at 2.58 Ma. *Journal of Quaternary Science* 25, 96–102.
- Hanken, N.-M., Bromley, R.G., Miller, J., 1996. Plio-Pleistocene sedimentation in coastal grabens, north-east Rhodes, Greece. *Geological Journal* 21, 271–296.
- Hansen, K.S., 1999. Development of a prograding carbonate wedge during sea level fall: lower Pleistocene of Rhodes, Greece. *Sedimentology* 46, 559–576.
- Hilgen, R.A., 1991. Astronomical calibration of Gauss to Matuyama sapropels in the Mediterranean and implication for the geomagnetic polarity time scale. *Earth and Planetary Science Letters* 104, 226–244.
- Hilgen, F.J., Lourens, L.J., Van Dam, J.A., 2012. The Neogene period. In: Gradstein, F.M., Ogg, J.G., Schmitz, M.D., Ogg, G.M. (Eds.), *The Geological Time Scale 2012*. Elsevier BV, Amsterdam, pp. 923–978.
- Jolivet, L., Faccenna, C., Huet, B., Labrousse, L., Le Pourtier, L., Lacombe, O., Lecomte, E., Burov, E., Denède, Y., Brun, J.-P., Philippon, M., Paul, A., Salaün, C., Karabulut, H., Piromallo, C., Monié, P., Gueydan, F., Okay, A.I., Oberhänsli, R., Pourteau, A., Augier, R., Gadenne, L., Driussi, O., 2013. Aegean tectonics: train localisation, slab tearing and trench retreat. *Tectonophysics* 597–598, 1–33.
- Kawagata, S., Hayward, B.W., Grenfell, H.R., Sabaa, A., 2005. Mid-Pleistocene extinction of deep-sea foraminifera in the North Atlantic Gateway (ODP sites 980 and 982). *Palaeogeography, Palaeoclimatology, Palaeoecology* 221, 267–291.
- Kennett, J.P., Srinivasan, M.S. (Eds.), 1983. *Neogene Planktonic Foraminifera, a Phylogenetic Atlas*. Hutchinson Ross Publishing Company, Stroudsburg, Pennsylvania, p. 265.
- Keraudren, B., 1970. Les formations quaternaires marines de la Grèce. *Bulletin du Musée d'Anthropologie préhistorique de Monaco* 6, 5–153.
- Koppers, A.A.P., 2002. ArCALC-software for $^{40}\text{Ar}/^{39}\text{Ar}$ age calculations. *Computers & Geosciences* 28, 605–619.
- Kovacs, E., Spjeldnaes, N., 1999. Pliocene-Pleistocene stratigraphy of Rhodes, Greece. *Newsletters on Stratigraphy* 37, 191–208.
- Lécuyer, C., Daux, V., Moissette, P., Cornée, J.-J., Quillévéré, F., Koskeridou, E., Fourel, F., Martineau, F., Reynard, B., 2012. Stable carbon and oxygen isotope compositions of invertebrate carbonate shells and the reconstruction of paleotemperatures and paleosalinities – a case study of the early Pleistocene of Rhodes, Greece. *Palaeogeography, Palaeoclimatology, Palaeoecology* 350–352, 39–48.
- Lekkas, E., Danamos, G., Skourtis, E., Sakellariou, D., 2001. Position of the Middle Triassic Tyros beds in the Gavrovo-Tripolis unit (Rhodes island, Dodecanese, Greece). *Geologica Carpathica* 53, 37–44.
- Lourens, L.J., Hilgen, F.J., Laskar, J., Shackleton, N.J., Wilson, D., 2005. The Neogene period. In: Gradstein, F.M., Ogg, J.G., Smith, A.G. (Eds.), *A Geological Time Scale 2004*. Cambridge University Press, pp. 409–440.
- Lourens, L.J., Hilgen, F.J., Raffi, I., 1998. Base of large *Gephyrocapsa* and astronomical calibration of early Pleistocene sapropels in Site 967 and Hole 969D: solving the chronology of the Vrica section (Calabria, Italy). In: Robertson, H.F., Emeis, K., Richter, C., et al. (Eds.), *Proceedings of the Ocean Drilling Program, Scientific Results*, 160, pp. 191–198 (College Station, TX).
- Lourens, L.J., Hilgen, F.J., Raffi, I., Vergnaud-Grassini, C., 1996. Early Pleistocene chronology of the Vrica section (Calabria, Italy). *Paleoceanography* 11 (6), 797–812.
- Løvlie, R., Støle, G., Spjeldnaes, N., 1989. Magnetic polarity stratigraphy of Pliocene–Pleistocene marine sediments from Rhodes, eastern Mediterranean. *Physics of the Earth and Planetary Interiors* 54, 340–352.
- Massari, F., Rio, D., Sgavetti, M., D'Alessandro, A., Asioli, A., Capraro, L., Fornaciari, E., Tatoe, F., 2002. Interplay between tectonics and glacio-eustasy: Pleistocene succession of the Crotone basin, Calabria (southern Italy). *Geological Society of America Bulletin* 114, 1183–1209.
- Matsuoka, H., Okada, H., 1990. Time-progressive morphometric changes of the genus *Gephyrocapsa* in the Quaternary sequence of the tropical Indian Ocean, site 709. In: Duncan, R.A., Backman, J., Peterson, L.C., et al. (Eds.), *Proceedings ODP, Scientific Results*, 115. Ocean Drilling Program, College Station, TX, pp. 255–270.
- McFadden, P.L., McElhinny, M.W., 1990. Classification of the reversal test in palaeomagnetism. *Geophysical Journal International* 103, 725–729.
- Meulenkamp, J.E., de Mulder, E.F.J., Van der Weerd, A., 1972. Sedimentary history and paleogeography of the Late Cenozoic of the Island of Rhodes. *Zeitschrift der Deutschen Geologischen Gesellschaft* 123, 541–553.
- Moissette, P., Spjeldnaes, N., 1995. Plio-Pleistocene deep-water bryozoans from Rhodes, Greece. *Palaeontology* 38, 771–799.
- Moissette, P., Koskeridou, E., Drinia, H., Cornée, J.-J., 2016. Facies associations in warm-temperate siliciclastic deposits: insights from early Pleistocene eastern Mediterranean (Rhodes, Greece). *Geological Magazine* 153, 61–83.
- Mutti, E., Orombelli, G., Pozzi, R., 1970. Geological studies on the Dodecanese Islands (Aegean Sea). IX. Geological map of the island of Rhodes (Greece); explanatory notes. *Annales Géologiques des Pays Helléniques* 22, 79–226.
- Narcisi, B., Vezzoli, L., 1999. Quaternary stratigraphy of distal tephra layers in the Mediterranean—an overview. *Global and Planetary Change* 21, 31–50.
- Nelson, C.S., Freiwald, A., Titschack, J., List, S., 2001. Lithostratigraphy and Sequence Architecture of Temperate Mixed Siliciclastic-carbonate Facies in a New Plio-Pleistocene Section at Plimiri, Rhodes Island (Greece), vol. 25. Department of Earth Sciences, University of Waikato, pp. 1–50. Occasional Reports.
- Nielsen, J.K., Hanken, N.-M., Nielsen, J.K., Hasen, K.S., 2006. Biostratigraphy and palaeoecology of the marine Pleistocene of Rhodes, Greece: Scleractinia, Serpulidae, Mollusca and Brachiopoda. *Bulletin of Geoscience* 81, 173–196.
- Orombelli, G., Montanari, C., 1967. Geological studies on the Dodecanese Islands (Aegean Sea): VI. The calabrian of the island of Rhodes (Greece), preliminary information. *Bulletino della Società Geologica Italiana* 86 (2), 103–113.
- Papanikolaou, M.D., Trianaphyllou, M.V., Platzman, E.S., Gibbard, P.L., Mac Niocaill, C., Head, M.J., 2011. A well-established early-middle Pleistocene marine sequence on south-east Zakynthos island, western Greece: magneto-biostratigraphic constraints and paleoclimatic implications. *Journal of Quaternary Science* 26 (5), 523–540.
- Pirazzoli, P.A., Montaggioni, L.F., Saliegue, J.F., Segonzac, G., Thommeret, Y., Vergnaud-Grassini, C., 1989. Crustal block movements from Holocene shorelines: Rhodes Island (Greece). *Tectonophysics* 170, 89–114.
- Raffi, I., Backman, J., Fornaciari, E., Pälike, H., Rio, D., Lourens, L., Hilgen, F., 2006. A review of calcareous nannofossil astrochronology encompassing the past 25 million years. *Quaternary Science Reviews* 25, 3113–3137.
- Raffi, I., Backman, J., Rio, D., Shackleton, N.J., 1993. Plio–Pleistocene nannofossil biostratigraphy and calibration to oxygen isotopes stratigraphies from deep sea drilling project site 607 and ocean drilling program site 677. *Paleoceanography* 3, 387–408.
- Rasmussen, T.L., Hastrup, A., Thomsen, E., 2005. Lagoon to deep-water foraminifera and ostracods from the Plio-Pleistocene Kallithea Bay section, Rhodes, Greece. In: Thomsen, E. (Ed.), *Cushman Foundation for Foraminiferal Research*, pp. 1–290. Special Publication 39.
- Renne, P.R., Swisher, C.C., Deino, A.L., Karner, D.B., Owens, T.L., DePaolo, J., 1998. Intercalibration of standards, absolute ages and uncertainties in $^{40}\text{Ar}/^{39}\text{Ar}$ dating. *Chemical Geology* 145, 117–152.
- Rio, D., 1982. The fossil distribution of Coccolithophore genus *Gephyrocapsa* Kamptner and related Plio-Pleistocene chronostratigraphic problems. In: Prell, W.L., Gardner, J.V., et al. (Eds.), *Initial Reports DSDP*, 68. US Govt. Printing Office, Washington, pp. 325–343.
- Rio, D., Raffi, I., Villa, G., 1990. Pliocene–Pleistocene calcareous nannofossil distribution patterns in the western Mediterranean. In: Kastens, K.A., Mascle, J., et al. (Eds.), *Proceedings of the ODP, Scientific Results*, 107. Ocean Drilling Program, College Station, TX, pp. 513–533.
- Samtleben, C., 1980. Die evolution der Coccolithophoriden-Gattung *Gephyrocapsa* nach Befunden im Atlantik. *Paläontologische Zeitschrift* 54, 91–125.
- Sissingh, W., 1972. Late Cenozoic Ostracoda of the south Aegean Island Arc. *Utrecht Micropaleontological Bulletins* 6, 1–187.
- Steinhorst, M., Lidgard, S., Hakansson, E., 2006. Reconstructing palaeoenvironments in a Pliocene–Pleistocene Mediterranean microbasin. *Facies* 52, 361–380.
- Ten Veen, J.H., Kleinspehn, K.L., 2002. Geodynamics along an increasingly curved convergent plate margin: Late Miocene–Pleistocene Rhodes, Greece. *Tectonics* 21, 1–21.
- Ten Veen, J.H., Boulton, S.J., Alçıcek, M.C., 2009. From palaeotectonics to neotectonics in the Neotethys realm: the importance of kinematic decoupling and inherited structural grain in SW Anatolia (Turkey). *Tectonophysics* 473, 261–281.
- Titschack, J., Joseph, N., Fietzke, J., Freiwald, A., Bromley, R.G., 2013. Record of a tectonically-controlled regression captured by changes in carbonate skeletal associations on a structured island shelf (mid-Pleistocene, Rhodes, Greece). *Sedimentary Geology* 283, 15–33.
- Titschack, J., Nelson, C.S., Beck, T., Freiwald, A., Radtke, U., 2008. Sedimentary evolution of a late Pleistocene temperate red algal reef (Coralligène) on Rhodes, Greece: correlation with global sea-level fluctuations. *Sedimentology* 55, 1747–1776.
- Titschack, J., Freiwald, A., 2005. Growth, deposition, and facies of Pleistocene bathyal coral communities from Rhodes, Greece. In: Freiwald, A., Roberts, J.M. (Eds.), *Cold-water Corals and Ecosystems*. Springer-Verlag Berlin Heidelberg, pp. 41–59.
- Thomsen, E., Rasmussen, T.L., Harstrup, A., 2001. Calcareous nannofossil, ostracode and foraminifera biostratigraphy of Plio-Pleistocene deposits, Rhodes (Greece), with a correlation to the Vrica section (Italy). *Journal of Micropaleontology* 20, 143–154.
- Tortorici, L., Caputo, R., Monaco, C., 2010. Late Neogene to Quaternary contractional structures in Crete (Greece). *Tectonophysics* 483, 203–213.
- van Hinsbergen, D.J.J., Krijgsman, W., Langereis, W., Cornée, J.-J., Duermeijer, C.E., Van Vugt, N., 2007. Discrete Plio-Pleistocene phases of tilting and counter-clockwise rotation in the southeastern Aegean arc (Rhodes, Greece): early Pliocene formation of the south Aegean left-lateral strike-slip system. *Journal of the Geological Society of London* 164, 1133–1144.

- van Hoof, A.A.M., Langereis, C.G., 1991. Reversal records in marine marls and delayed acquisition of remanent magnetization. *Nature* 351, 223–224.
- Vasiliev, I., Franke, C., Meeldijk, J.D., Dekkers, M.J., Langereis, C.G., Krijgsman, W., 2008. Putative greigite magnetofossils from the Pliocene epoch. *Nature Geoscience* 1 (11), 782–786.
- Weinholz, P., Lutze, G.F., 1989. The Stilostomella extinction. In: Baldauf, J., Heath, G.G., Ruddiman, W.F., Sarnthein, M. (Eds.), *Proceedings of the ODP, Scientific Results*, vol. 108. Ocean Drilling Program, College Station, TX, pp. 113–117.